Electronic Supplementary Material (ESI) for Analytical Methods.

Supporting Information

X-ray structure of two Schiff bases: TURN-ON sensing of Fe^{3+} and Al^{3+} insight the HepG2 cell line

Sunanda Dey, Suvendu Maity, Rakesh Purkait, Kunal Pal, Prasanta Ghosh, Kuladip Jana, and Chittaranjan Sinha*

Sl. No.	Contents	Fig./ Scheme/ Table No.
1.	**Experimental section:** Materials and methods	
2.	Calculation of Limit of Detection (LOD) and Quantum yield	
3.	Common methods for UV-Vis and fluorescence measurements	
4.	Preparation of [Fe(**L'**)Cl_2]	
5.	Preparation of Al complex, [Al(**L"**)(NO_3)(OH_2)]	
6.	Cell line culture, Cell Imaging and Cell survivability assay	
7.	^{1}H NMR spectrum of probe **HL'** in DMSO-d_6 (400 MHz).	Fig. S1
8.	^{13}C NMR spectrum of probe **HL'** in DMSO-d_6 (400 MHz).	Fig. S2
9.	ESI-MS spectrum of probe **HL'**.	Fig. S3
10.	FT-IR spectrum of probe **HL'**.	Fig. S4
11.	^{1}H NMR spectrum of probe **H_2L"** in DMSO-d_6 (500 MHz).	Fig. S5
12.	^{13}C NMR spectrum of probe **H_2L"** in DMSO-d_6 (500 MHz).	Fig. S6
13.	ESI-MS spectrum of probe **H_2L"**.	Fig. S7
14.	FT-IR spectrum of probe **H_2L"**.	Fig. S8
15.	Crystal data and refinement parameters for probe **HL'** and **H_2L"**.	Table S1
16.	Some important bond length and bond angles of **HL'**.	Table S2
17.	Some important bond length and bond angles of **H_2L"**.	Table S3
18.	Supramolecular interactions present in the probe **HL'**.	Fig. S9
19.	Supramolecular interactions present in the probe **H_2L"**.	Fig. S10
20.	Job's plot for determination of binding stoichiometry (a) **HL'** with Fe^{3+}; (b) **H_2L"** with Al^{3+}.	Fig. S11
21.	ESI-MS spectrum of [Fe(**L'**)$(Cl)_2$] complex.	Fig. S12

22.	ESI-MS spectrum of [Al(**L"**)(NO_3)(OH_2)] complex.	Fig. S13
23.	FT-IR spectrum of [Fe(**L'**)($Cl)_2$] complex.	Fig. S14
24.	FT-IR spectrum of [Al(**L"**)(NO_3)(OH_2)] complex.	Fig. S15
25.	Emission Intensity of probes in different solvents (a) **HL'** and (b) **H_2L"**.	Fig. S16
26.	Proton transfer of **HL'** in excited state	Scheme S1
27.	Tautomerisation of **H_2L"** in excited state	Scheme S2
28.	Benesi-Hildebrand plot for determination of binding constant of probes with metal ions in H_2O (HEPES buffer, pH 7.4) (a) **HL'** with Fe^{3+} (b) **H_2L"** with Al^{3+}.	Fig. S17
29.	LOD determination by following 3σ/m method (a) Fe^{3+} for probe **HL'** (b) Al^{3+} for **H_2L"**.	Fig. S18
30.	Fluorescence lifetime spectra in H_2O (HEPES buffer, pH 7.4) (a) **HL'** and **HL'** with Fe^{3+} (b) **H_2L"** and **H_2L"** with Al^{3+}.	Fig. S19
31.	Dependence of emission intensity for the probes on pH in the absence and presence of selective metal ions in H_2O (HEPES buffer, pH 7.4) (a) **HL'** and **HL'** with Fe^{3+} (b) **H_2L"** and **H_2L"** with Al^{3+}.	Fig. S20
32.	Interference of various metal ions (a) Fe^{3+} sensitivity for **HL'** (b) Al^{3+} for **H_2L"**.	Fig. S21
33.	Emission spectral changes of probes (50 μM) upon addition of various anions (100 μM) in H_2O (HEPES buffer, pH 7.4) (a) **HL'**, λ_{ex}=300 nm; (b) **H_2L"**, λ_{ex}=400 nm.	Fig. S22
34.	Effect of temperature in fluorescence intensity of **HL'**.	Fig. S23
35.	Effect of temperature in fluorescence intensity of **HL'**+Fe^{3+}.	Fig. S24
36.	Effect of temperature in fluorescence intensity of **H_2L"**.	Fig. S25
37.	Effect of temperature in fluorescence intensity of **H_2L"**+Al^{3+}.	Fig. S26

Experimental section

Materials and methods

2-benzoyl pyridine, o-Phenylenediamine, Thiophene-2-carboxaldehyde and 2-Hydroxy-1-naphthaldehyde were obtained from Sigma-Aldrich and used as received. All the other reagents were bought from commercial sources and used without further purification. Before using the solvents for spectroscopic studies these were dried by standard procedures.[1] NMR spectra of the synthesized compounds were taken by Bruker 500 MHz (for **H_2L"**) and 400 MHz (for **HL'**) spectrometer using TMS as an internal standard. FT-IR spectra were recorded by Perkin Elmer RX-1 FTIR spectrophotometer (KBr disk, 4000–400 cm^{-1}). For elemental analysis, PerkinElmer Series-II CHN analyser (2400) was used. The mass spectra of the compounds were collected from a Water HRMS spectrometer (XEVO-G2QTOF#YCA351). The absorbance and emission spectra were recorded by using Perkin Elmer Lambda 25 spectrophotometer and Perkin Elmer Spectrofluorimeter of model LS55 respectively. The fluorescence lifetime measurements were taking by using time-correlated single photon counting (TCSPC) setup from Horiba Jobin Yvon.

Calculation of Limit of Detection (LOD) and Quantum yield

The limit of detection (LOD) was calculated from the fluorescence titration measurement obtained by gradual addition of metal ions to the probe solution. For the determination of standard deviation the emission intensity of the free probes (without any analyte) were measured by varying the concentration. The limit of detection of probes for Fe^{3+} and Al^{3+} were determined by following equation: LOD = 3 σ/m and σ = standard deviation; m = slope of the calibration curve obtained from fluorescence titration measurement by adding selective metal ions to the probe solution.

Fluorescence quantum yields (Φ) were obtained by using the equation:

$\Phi_{sample} = (OD_{std.} \times A_{sample})/(OD_{sample} \times A_{std.}) \times \Phi_{std.}$

Where, A_{sample} and $A_{std.}$ represent the areas under the fluorescence spectral curves. The optical densities of the sample and standard are labelled as OD_{sample} and $OD_{std.}$, respectively (at the excitation wavelength). Here, acidic quinine sulfate was taken as the standard ($\Phi_{std.} = 0.54$) for the quantum yield calculation of probes **HL'**, **H_2L"**, **HL'**+Fe^{3+} and **H_2L"**+Al^{3+}.

Common methods for UV-Vis and fluorescence measurements

For UV-Vis as well as fluorescence measurements 1.0×10^{-3} M stock solution of probes was prepared by dissolving the probes (as required) in MeOH solution. All the required metal cation of 1.0×10^{-3} M solution was prepared in deionized water. For checking sensitivity, selectivity and all the UV-Vis as well as fluorescence measurements towards metal cations, 50 μM main solution was prepared in H_2O (HEPES buffer, pH 7.4) by taking the above stock solution and into this solution 1.00 equivalent metal salt used.

Preparation of [Fe(**L'**)Cl_2]

15 mL methanol solution of $FeCl_3.6H_2O$ (0.270 g, 1 mmol) was added to **HL'** (0.37 g, 1 mmol) in 10 mL methanol, stirred for 7 h and the solution was permitted to evaporate very slowly. After five days a deep green crystalline product was obtained and used for characterization (ESI-MS and FTIR).

Preparation of Al complex, [Al(**L"**)(NO_3)(OH_2)]

To 15 mL MeOH solution of **H_2L"** (0.43 g, 1 mmol), $Al(NO_3)_3.9H_2O$ (0.38 g, 1 mmol) was added (in methanol, 10 mL), stirred for 6 h and then the solution was allowed to evaporate very

slowly. After few days a brown coloured crystalline product was obtained and used for various spectroscopic characterizations (ESI-MS and FTIR).

Cell line culture

Human liver cancer cell line, HepG2 and human lung fibroblast cells, WI-38 were obtained from National Center for Cell Science (NCCS) Pune, India. The cells were grown in DMEM with 10% Fetal Bovine Serum (FBS), penicillin/streptomycin (100 units/ml) at 37ºC and 5% CO_2. All the treatments were accompanied at 37ºC and at a cell density permitting exponential growth.

Cell Imaging

The HepG2 cells were grown in coverslips for 24 h. Then the cells were either mock-treated or treated with 10 µM of probes (**HL'** and **H_2L"**) and 10 µM salts (Fe^{3+} and Al^{3+}) were incubated for 24 h at 37ºC.[2] The cells were washed with 1×PBS. Then they were mounted on a glass slide and observed under fluorescence microscope (Leica).

Cell survivability assay

Cell survivability of the probes (**HL'** and **H_2L"**) was studied for human lung fibroblast cells, WI-38 by following previously reported procedure.[3] In shortly, viability of WI-38 cells after exposure to various concentrations of probes was assessed by MTT assay. The cells were seeded in 96-well plates at 1×10^4 cells per well and exposed to probes at concentrations of 0 µM, 20 µM, 40 µM, 60 µM, 80 µM, 100 µM for 24 h. After incubation cells were washed with 1×PBS twice and incubated with MTT solution (450 µg/ml) for 3-4 h at 37ºC. The resulting formazan crystals were dissolved in an MTT solubilization buffer and the absorbance was measured at 570 nm by using a spectrophotometer (BioTek) and the value was compared with control cells.

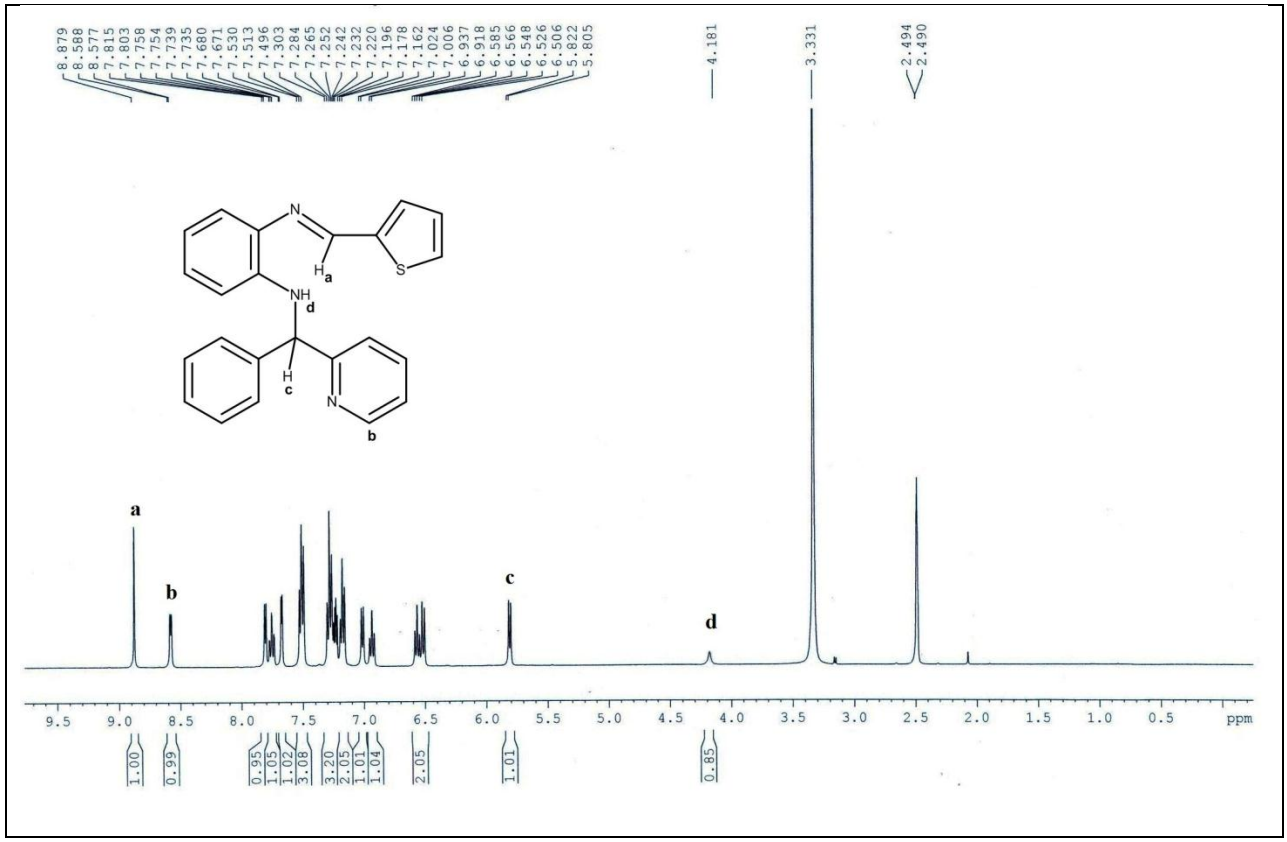

Fig. S1. ^{1}H NMR spectrum of probe **HL'** in DMSO-d_6 (400 MHz).

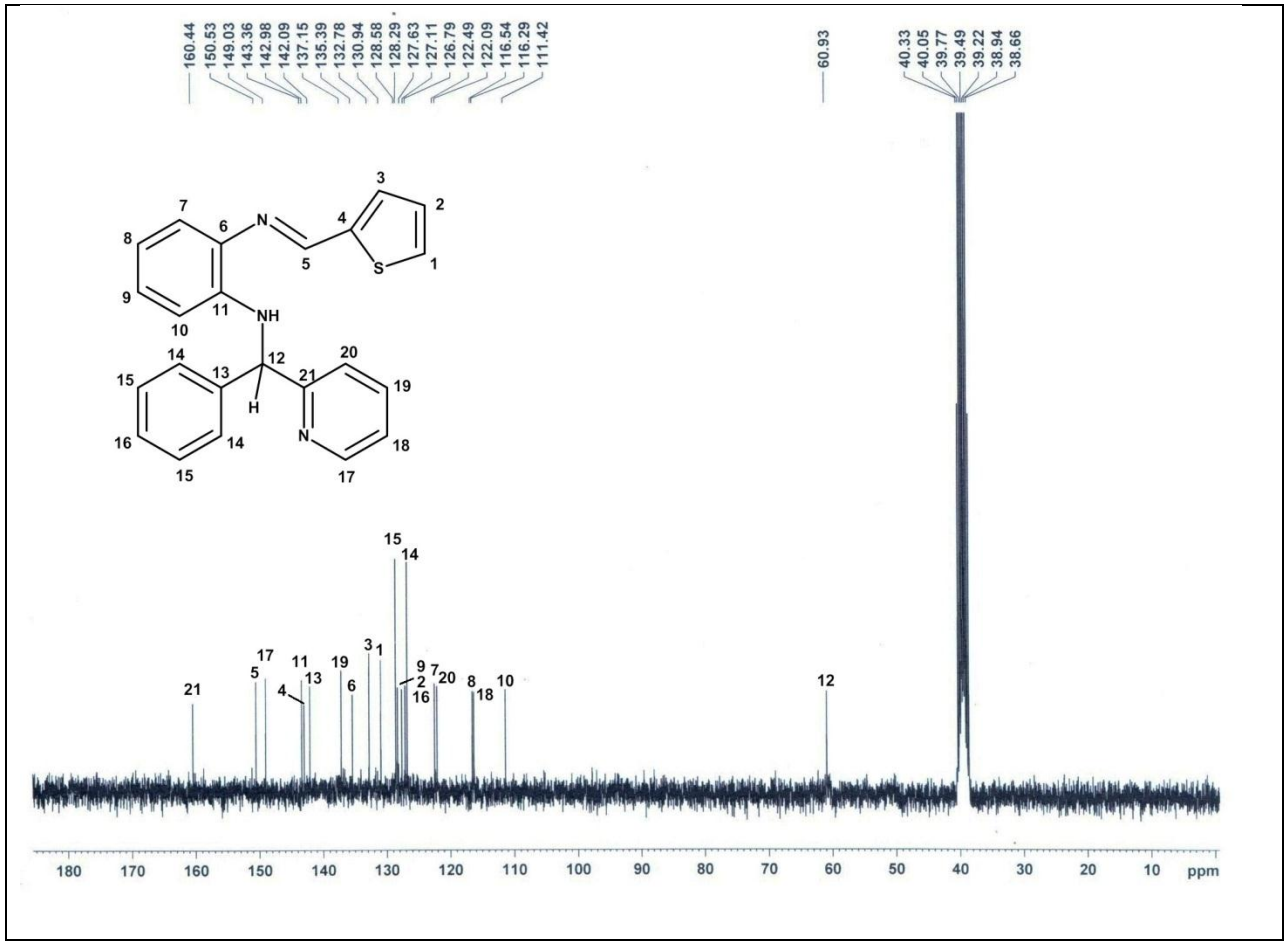

Fig. S2. ^{13}C NMR spectrum of probe **HL'** in DMSO-d_6 (400 MHz).

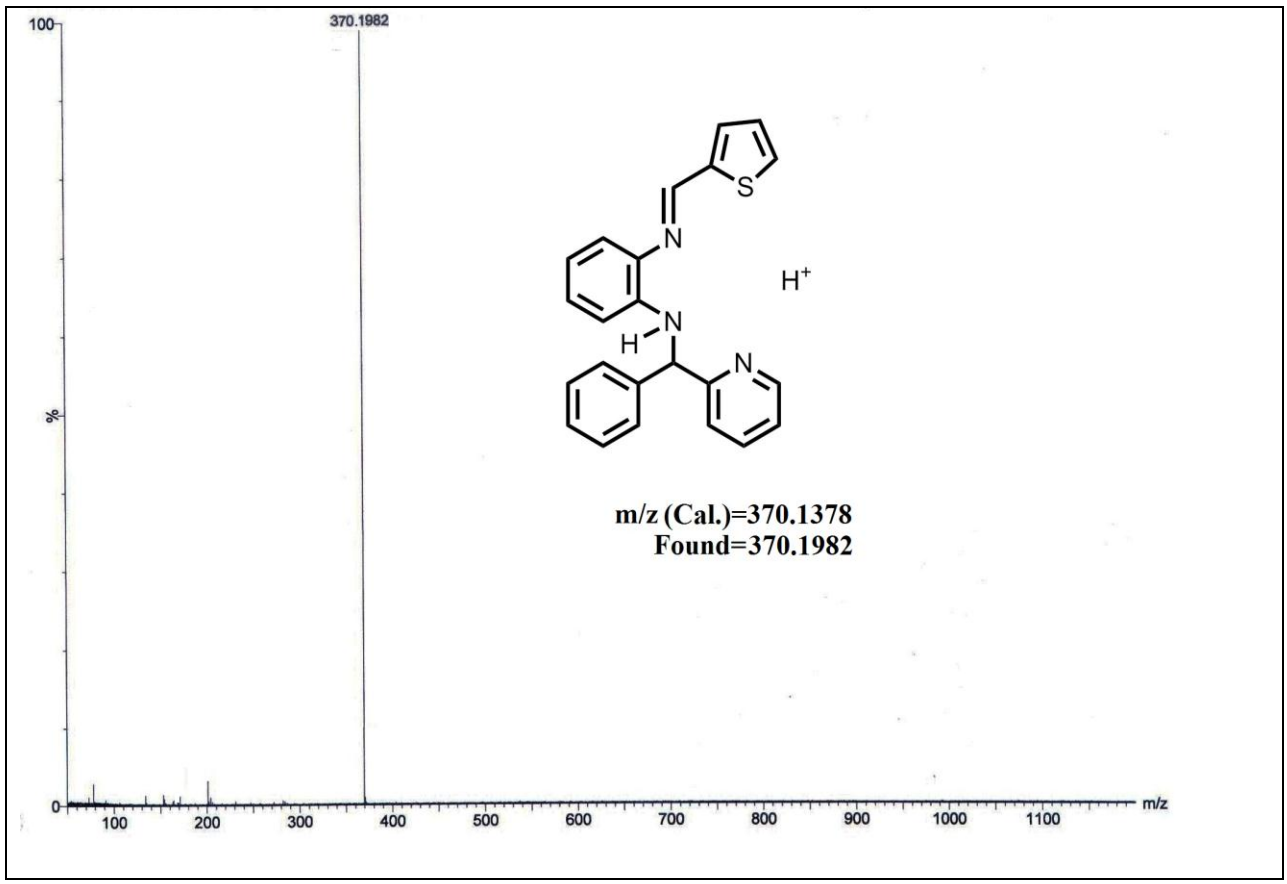

Fig. S3. ESI-MS spectrum of probe **HL'**.

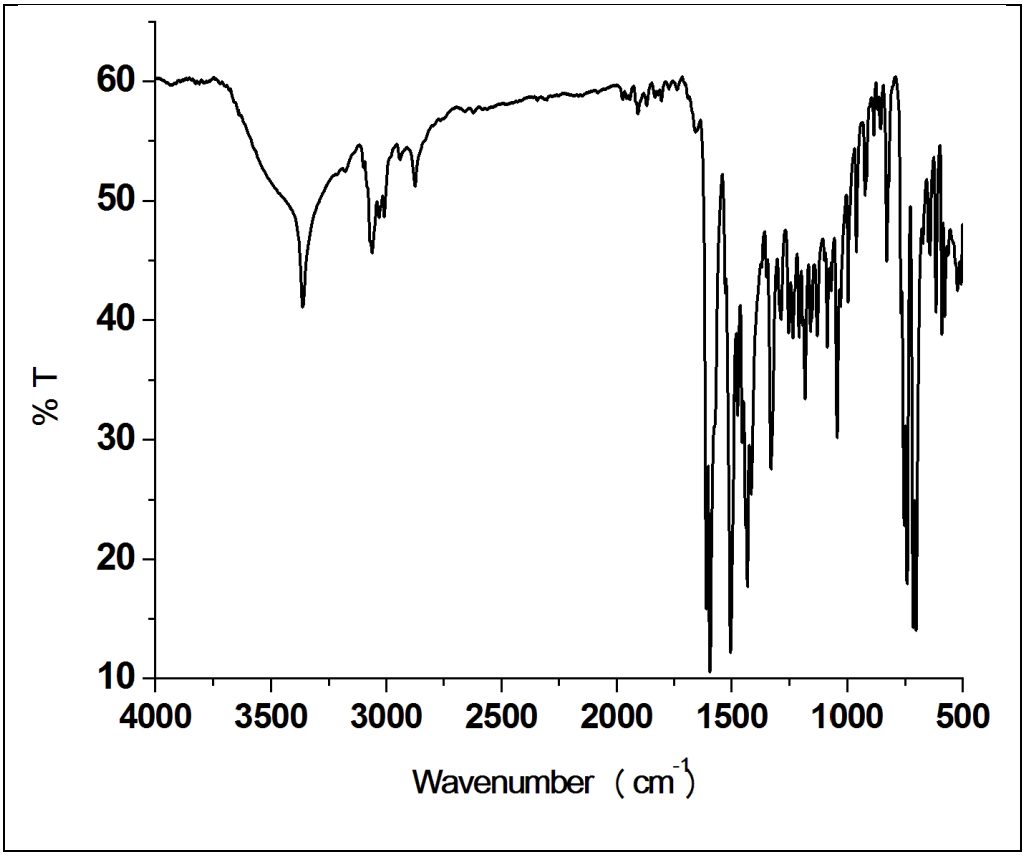

Fig. S4. FT-IR spectrum of probe **HL'**.

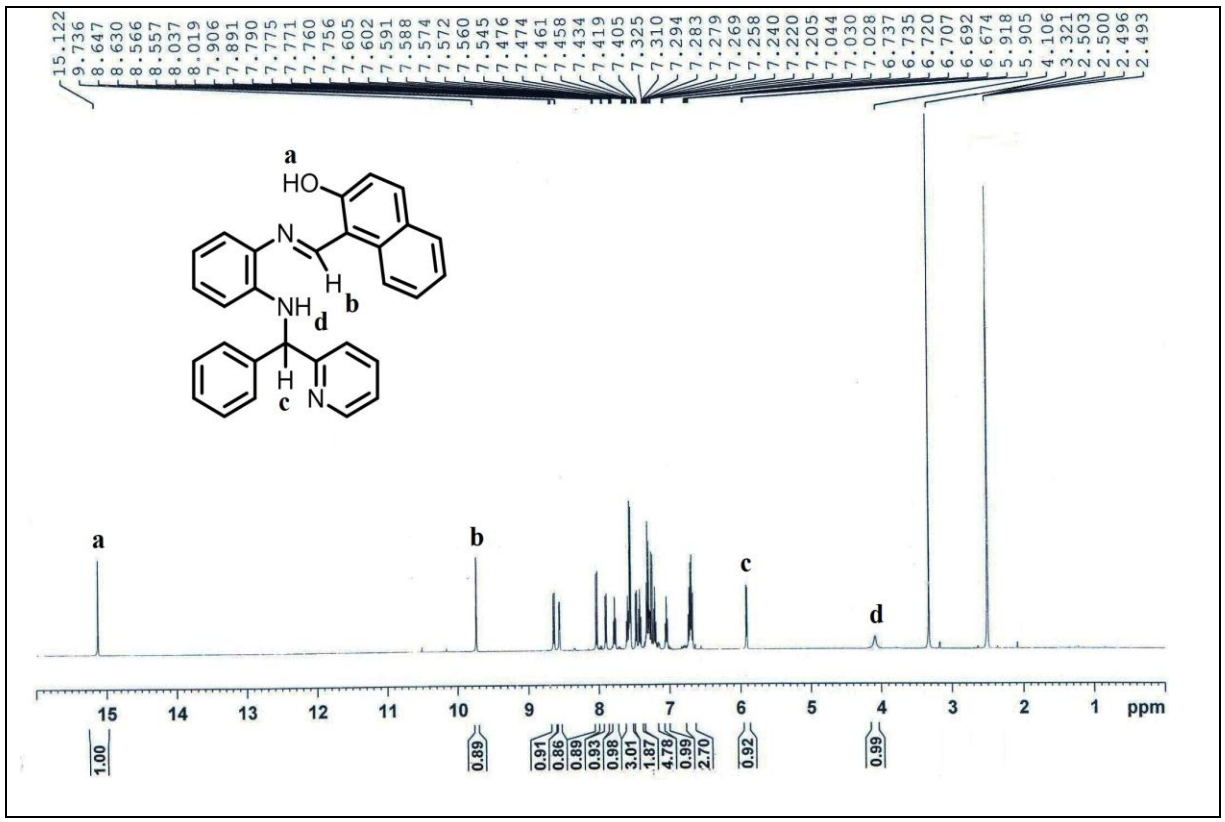

Fig. S5. ^{1}H NMR spectrum of probe **H_2L"** in DMSO-d_6 (500 MHz).

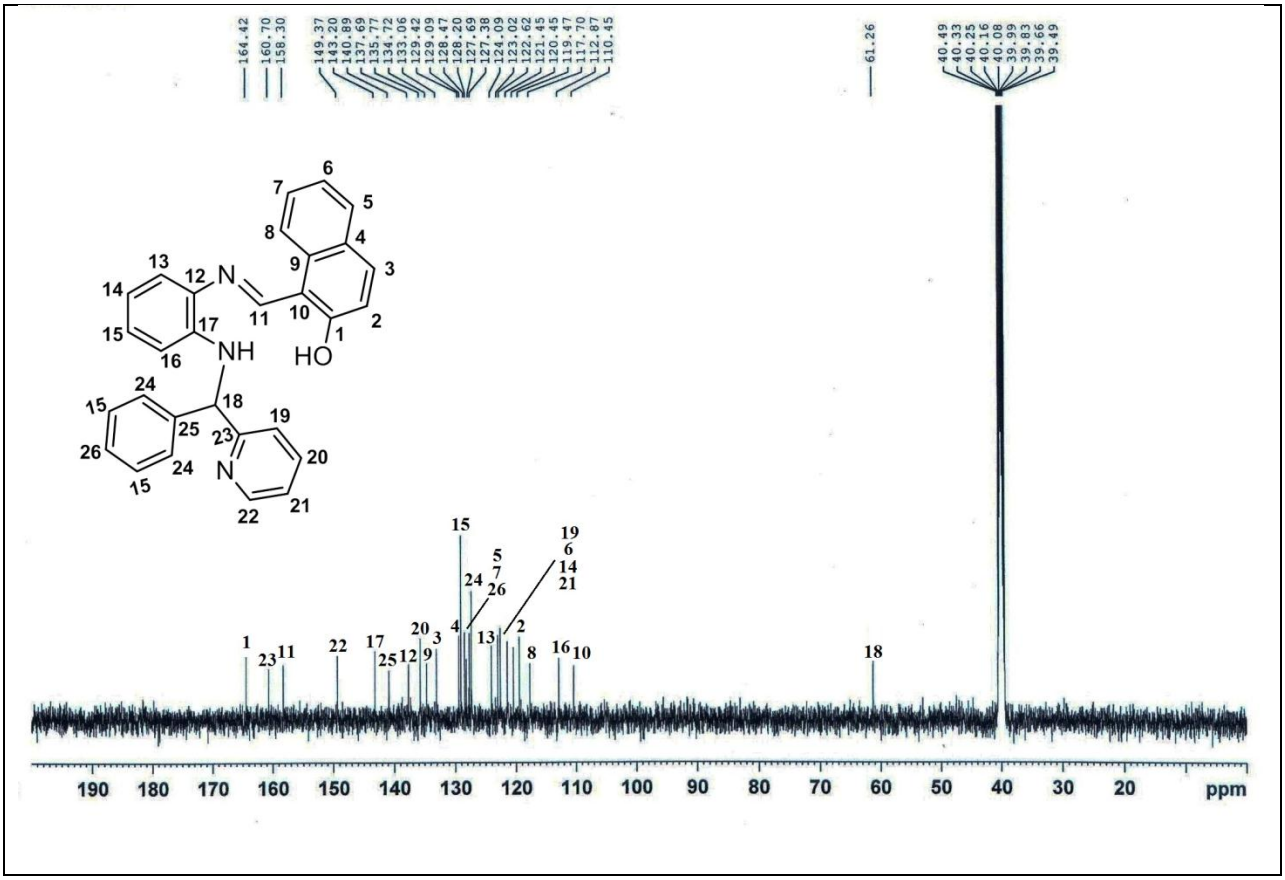

Fig. S6. ^{13}C NMR spectrum of probe **H_2L"** in DMSO-d_6 (500 MHz).

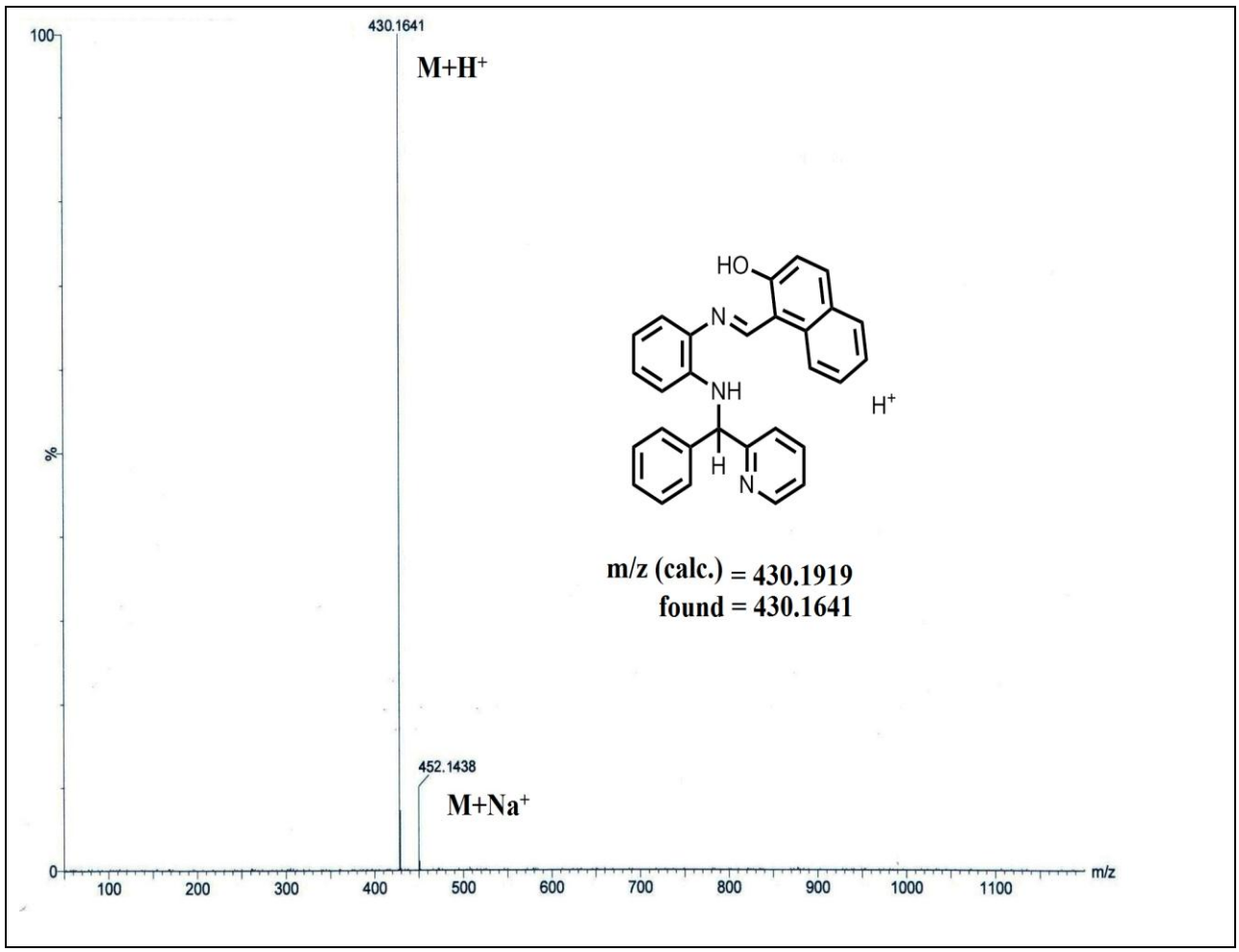

Fig. S7. ESI-MS spectrum of probe **H_2L"**.

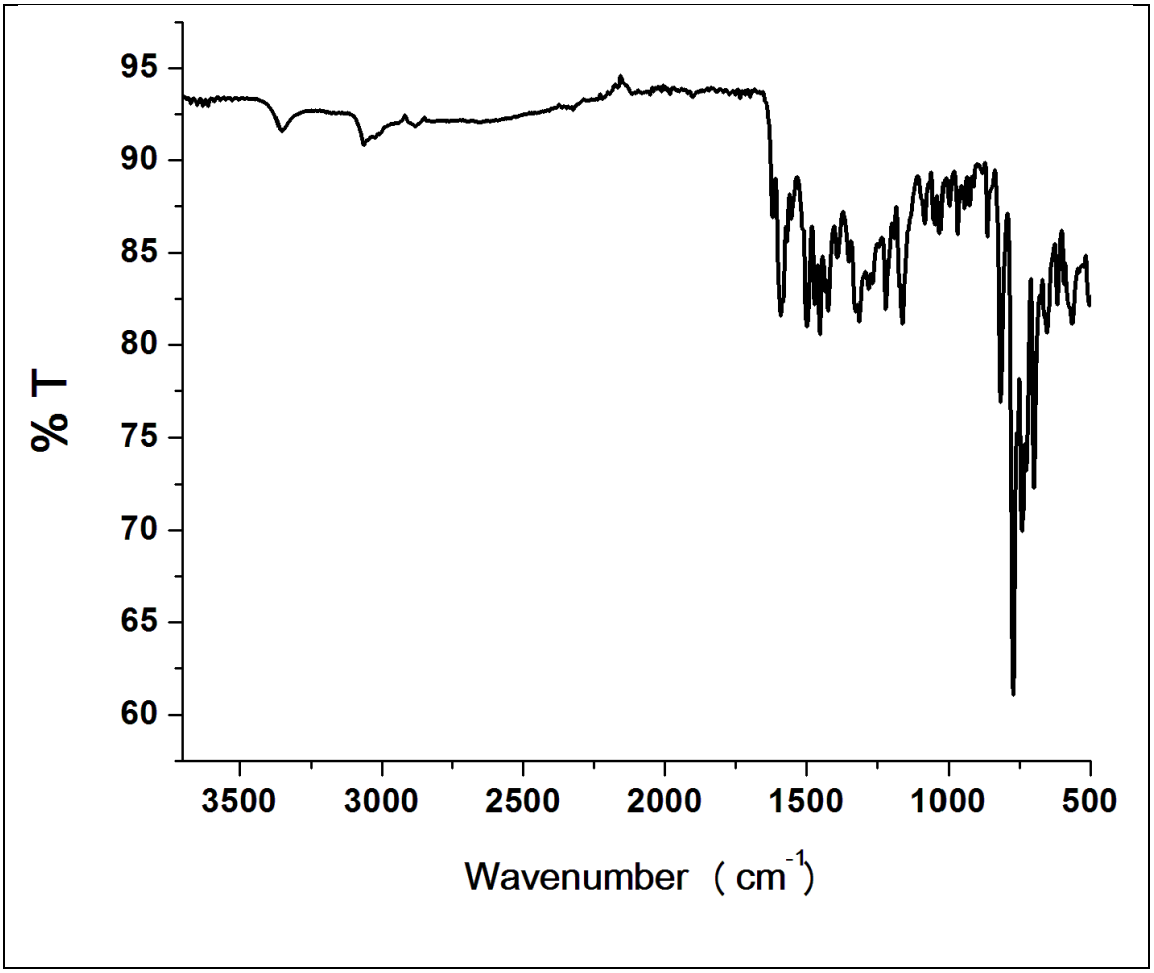

Fig. S8. FT-IR spectrum of probe **H_2L"**.

Table S1 Crystal data and refinement parameters for probe **HL'** and **H_2L"**.

	HL'	**H_2L"**
Formula	$C_{23}H_{19}N_3S$	$C_{29}H_{23}N_3O$
fw	369.47	429.50
Crystal System	monoclinic	monoclinic
Space group	P 21/c	P 21/c
a (Å)	9.8094(3)	22.180(3)

b (Å)	20.7167(7)	5.9098(7)
c (Å)	9.6437(3)	16.938(2)
α=γ/°	90	90
β/°	93.5560(10)	94.383(4)
V $(Å)^3$	1956.00(11)	2213.7(5)
Z	4	4
Dc/g cm^{-3}	1.255	1.289
μ/mm^{-1}	0.177	0.079
λ(Å)	0.71073	0.71073
data[$I > 2\sigma(I)$]/params	3998/244	3882/299
GOF[c]	1.031	1.138
final R indices [$I > 2\sigma(I)$][a,b]	R1 = 0.0534 wR2 = 0.1561	R1 = 0.0913 wR2 = 0.1730

[a] $R_1 = \Sigma||F_o|-|F_c||/\Sigma|F_o|$; [b] $wR_2 = \{\Sigma[w(F_o^2-F_c^2)^2]/\Sigma[w(F^2_o)^2]\}^{1/2}$; $w = [\sigma^2(F_o)^2 + (0.1003P)^2 + 4.9693P]^{-1}$ $(F_o^2 + 2F_c^2)/3$; [c] Goodness-of-fit

Table S2 Some important bond length and bond angles of **HL'**.

Bond	**Length/Angle (Å/°)**	**Bond**	**Angle (°)**
S(1) - C(14)	1.716(2)	C(14) - S(1) - C(17)	90.96(13)
N(2) - C(6)	1.446(2)	C(12) - N(3) - C(13)	119.54(17)
C(5) - C(6)	1.519(3)	N(1) - C(5) - C(6)	117.60(17)

C(13) - C(14)	1.435(3)	N(2) - C(6) - C(18)	112.42(17)
N(2) - H(2)	0.86	N(2) - C(7) - C(12)	117.77(17)
S(1) - C(17)	1.706(3)	N(3) - C(12) - C(7)	116.68(17)
N(2) - C(7)	1.373(3)	N(3) - C(13) - C(14)	122.03(18)
C(6) - C(18)	1.519(3)	C(13) - C(14) - C(15)	127.5(2)
C(14) - C(15)	1.386(3)	S(1) - C(17) - C(16)	112.8(2)
C(6) - H(6)	0.98	C(6) - N(2) - H(2)	118
N(1) - C(1)	1.347(3)	C(5) - C(4) - H(4)	121
N(3) - C(12)	1.409(3)	N(3) - C(13) - H(13)	119
C(7) - C(8)	1.390(3)	S(1) - C(17) - H(17)	124
C(13) - H(13)	0.93	N(1) - C(1) - C(2)	123.5(3)
N(1) - C(5)	1.326(3)	C(5) - C(6) - C(18)	110.59(16)
N(3) - C(13)	1.269(3)	N(3) - C(12) - C(11)	124.22(19)
C(7) - C(12)	1.417(3)	S(1) - C(14) - C(13)	121.26(16)
C(14) - C(15) - C(16)	112.0(2)	N(2) - C(6) - H(6)	108
C(6) - C(18) - C(19)	121.86(19)	C(7) - C(8) - H(8)	120
C(7) - N(2) - H(2)	118	C(14) - C(13) - H(13)	119
C(6) - N(2) - C(7)	123.49(17)	C(7) - C(12) - C(11)	119.04(19)
N(1) - C(5) - C(4)	122.3(2)	S(1) - C(14) - C(15)	111.29(17)
N(2) - C(6) - C(5)	109.71(16)	C(6) - C(18) - C(23)	119.95(18)
N(2) - C(7) - C(8)	123.65(18)	N(1) - C(1) - H(1)	118
C(7) - C(8) - C(9)	120.69(19)	C(5) - C(6) - H(6)	108

Table S3 Some important bond length and bond angles of **H_2L"**.

Bond	**Length/Angle (Å/°)**	**Bond**	**Angle (°)**
O1 - C3	1.332(5)	C1 - N1 - C12	122.1(3)
N003 - C18	1.437(5)	N1 - C1 - C2	123.3(3)
C2 - C3	1.390(5)	C3 - C2 - C11	118.9(3)
C12 - C17	1.384(6)	C2 - C3 - C4	121.0(4)
O1 - H1	0.82	C13 - C12 - C17	118.7(4)
N1 - C1	1.286(5)	C12 - C13 - C14	118.5(3)
N2 - C25	1.336(6)	N003 - C18 - C25	108.9(3)
C2 > C11	1.442(5)	C18 - C19 - C24	119.6(3)
C13 - C14	1.390(5)	C18 - C25 - C28	120.4(4)
C18 - C19	1.527(5)	C3 - O1 - H1	109
C25 - C28	1.374(6)	N1 - C1 - H1A	118
N003 - H003	0.86	C25 - C18 - H18	108
C18 - H18	0.98	C13 - N003 - C18	124.1(3)
N1 - C12	1.419(5)	C1 - C2 - C3	120.0(3)
N2 - C27	1.361(8)	O1 - C3 - C2	122.2(4)
C3 - C4	1.407(6)	C3 - C4 - C5	120.1(4)
C18 - C25	1.526(5)	C2 - C11 - C6	119.0(3)
C1 - H1A	0.93	N1 - C12 - C13	117.0(3)
N003 - C13	1.381(5)	N003 - C13 - C12	119.9(3)

C1 > C2	1.442(5)	C13 - C14 - C15	121.2(4)
C12 - C13	1.405(5)	C12 - C17 - C16	121.8(4)
N2 - C25 - C18	116.9(3)	N2 - C27 - C30	124.1(6)
C13 - N003 - H003	118	C2 - C1 - H1A	118
N003 - C18 - H18	108	C25 - C28 - H28	120
C25 - N2 - C27	116.1(4)	C1 - C2 - C11	121.0(3)
O1 - C3 - C4	116.9(3)	C2 - C11 - C10	123.8(4)
N1 - C12 - C17	124.3(4)	N003 - C13 - C14	121.7(3)
N003 - C18 - C19	113.4(3)	C18 - C19 - C20	121.8(4)
N2 - C25 - C28	122.7(4)	C25 - C28 - C29	119.2(5)
C18 - N003 - H003	118	C3 - C4 - H4	120
C13 - C14 - H14	119	C12 - C17 - H17	119
N2 - C27 - H27	118		

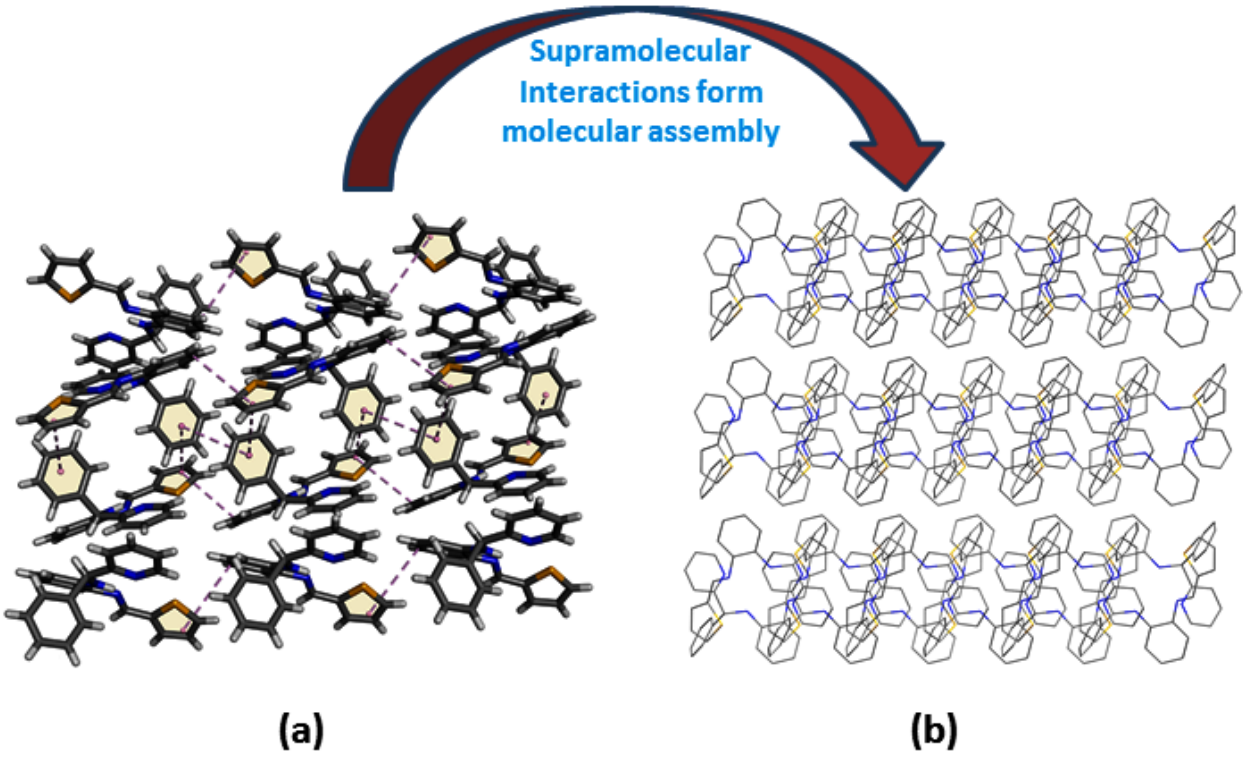

Fig. S9. Supramolecular interactions present in the probe **HL'**.

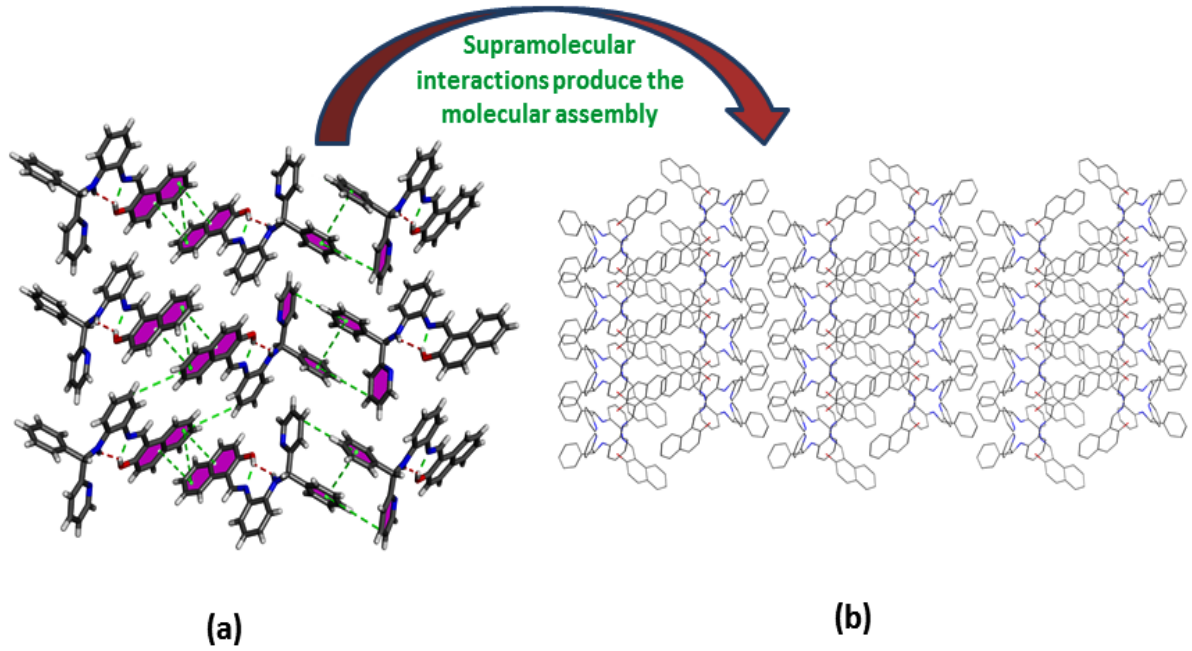

Fig. S10. Supramolecular interactions present in the probe **H_2L''**.

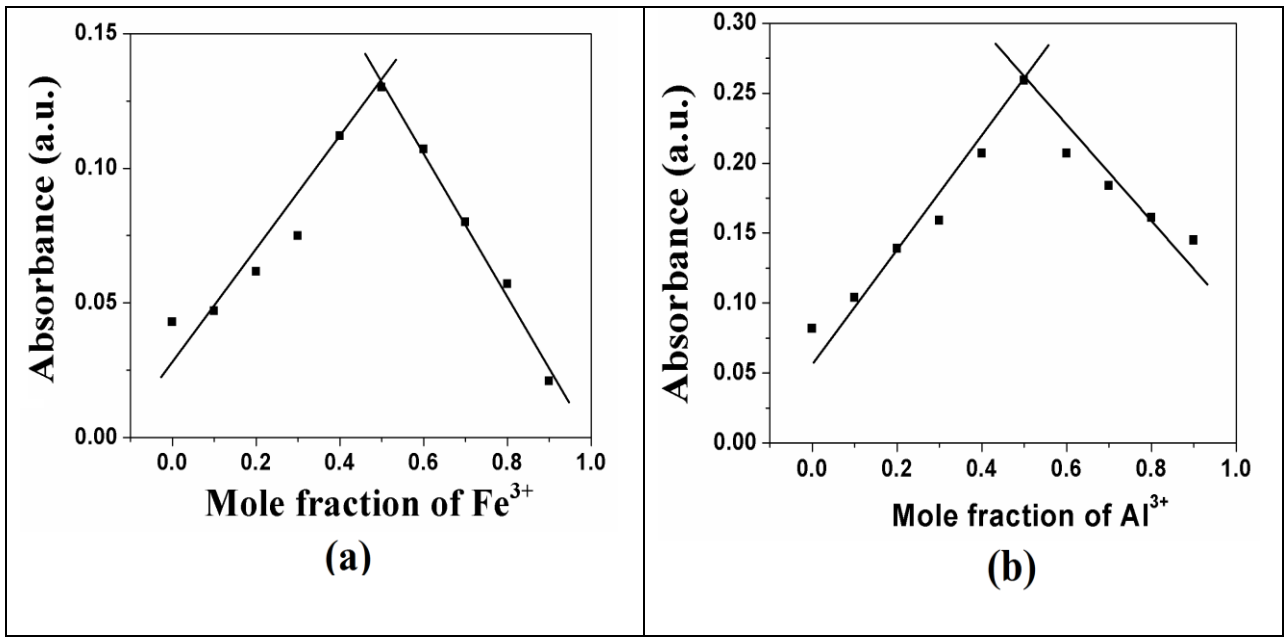

Fig. S11. Job's plot for determination of binding stoichiometry (a) **HL'** with Fe^{3+}; (b) **H_2L"** with Al^{3+}.

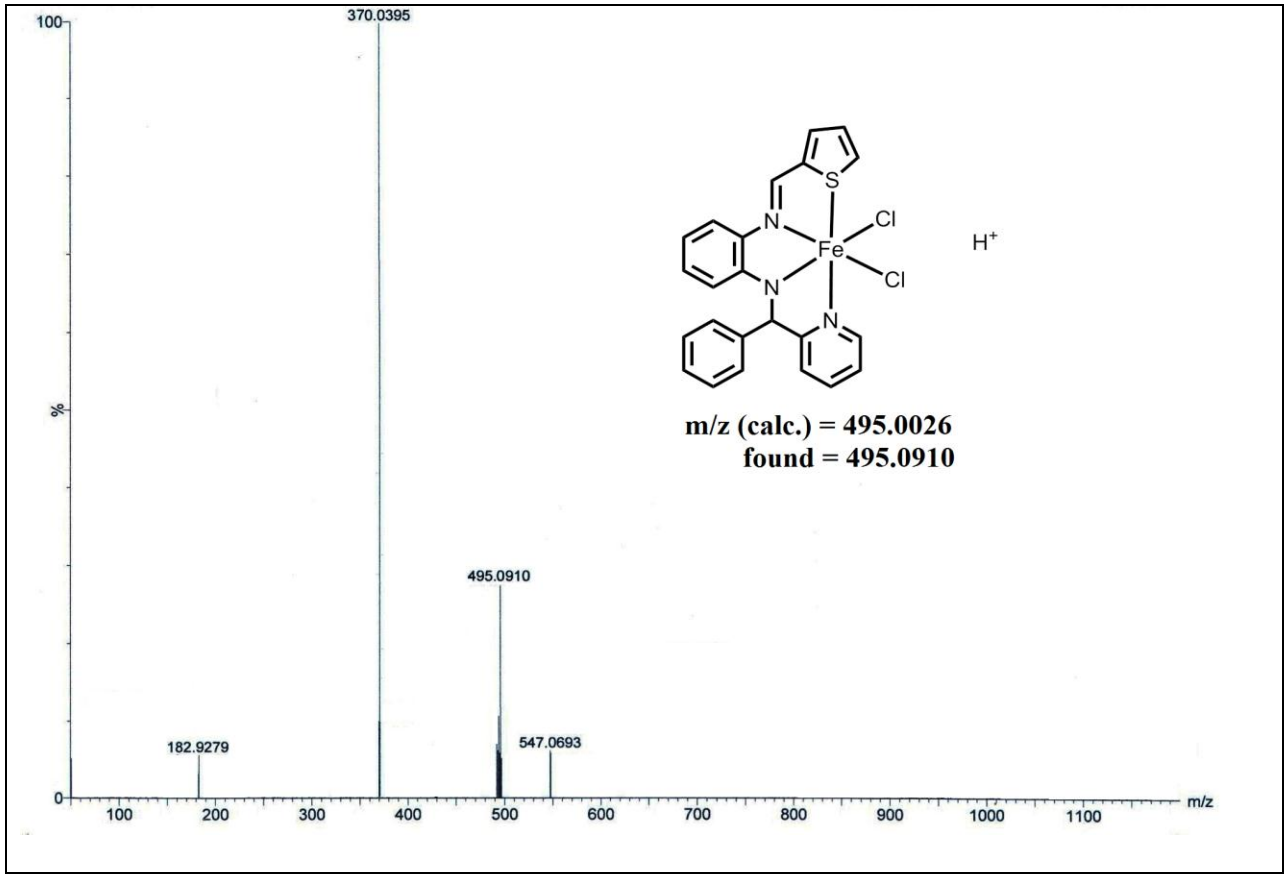

Fig. S12. ESI-MS spectrum of [Fe(**L'**)$(Cl)_2$] complex.

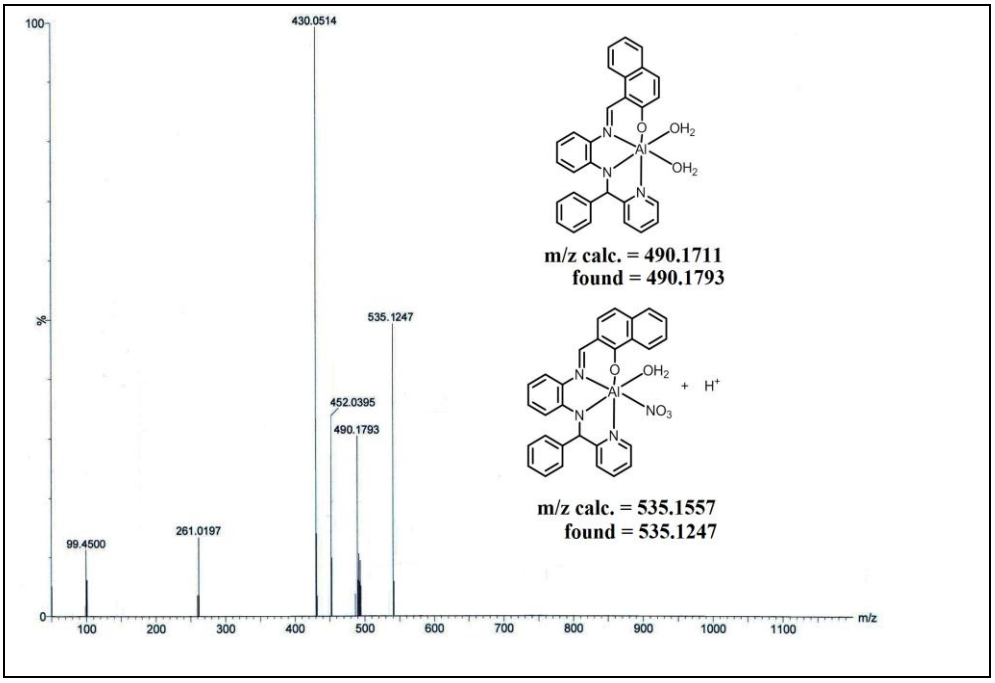

Fig. S13. ESI-MS spectrum of [Al(**L"**)(NO_3)(OH_2)] complex.

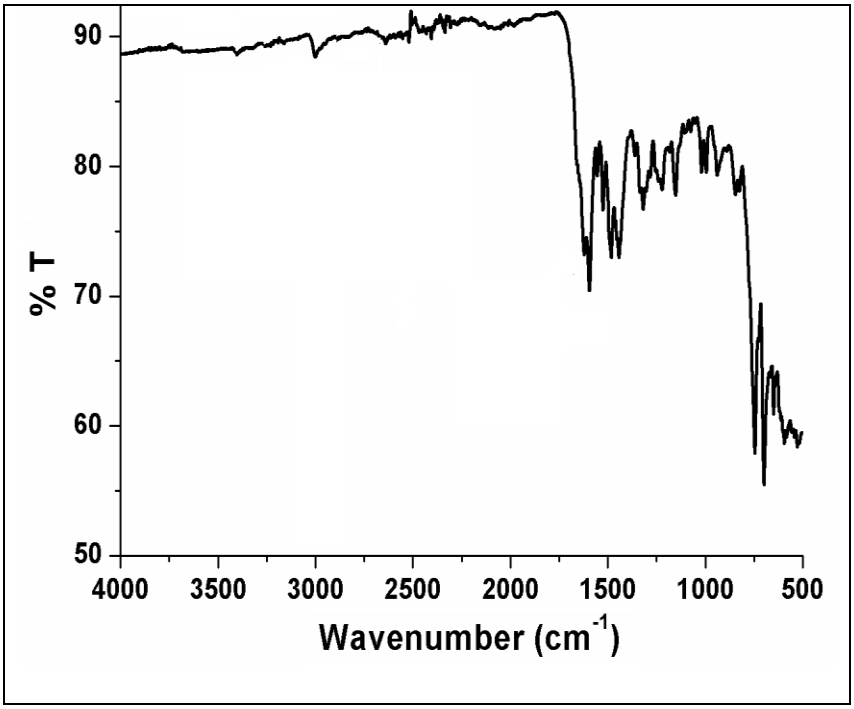

Fig. S14. FT-IR spectrum of [Fe(**L'**)$(Cl)_2$] complex.

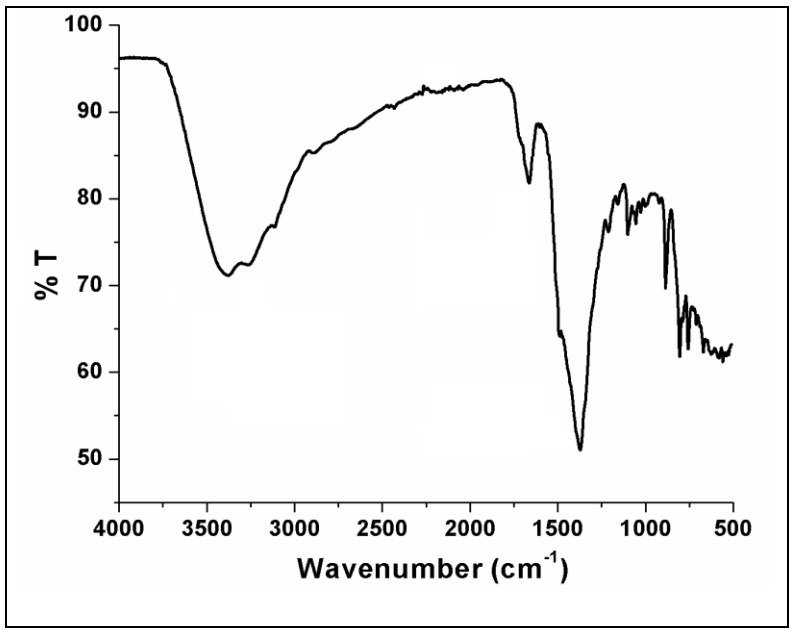

Fig. S15. FT-IR spectrum of [Al(**L"**)(NO_3)(OH_2)] complex.

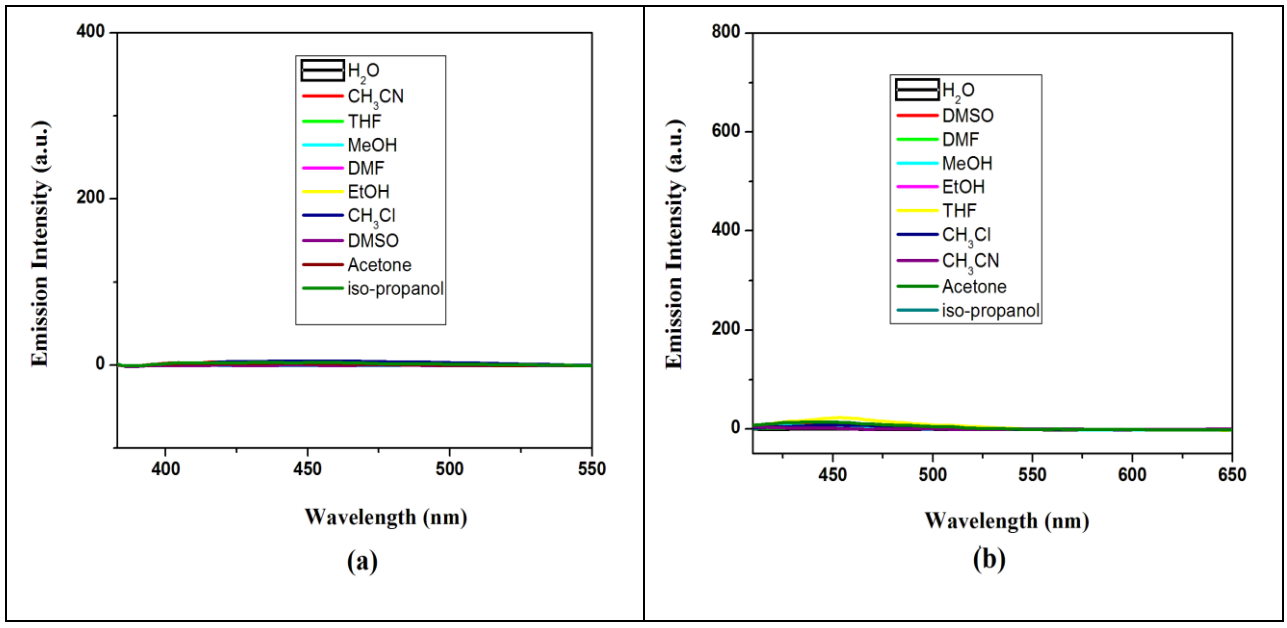

Fig. S16. Emission Intensity of probes in different solvents (a) **HL'** and (b) **H_2L"**.

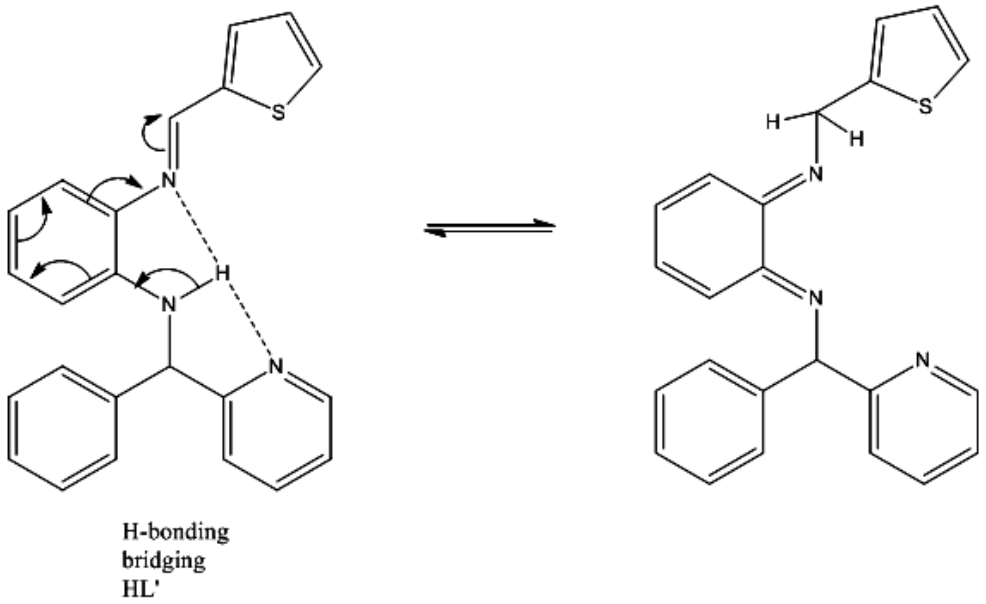

H-bonding
bridging
HL'

Scheme S1 Proton transfer of **HL'** in excited state

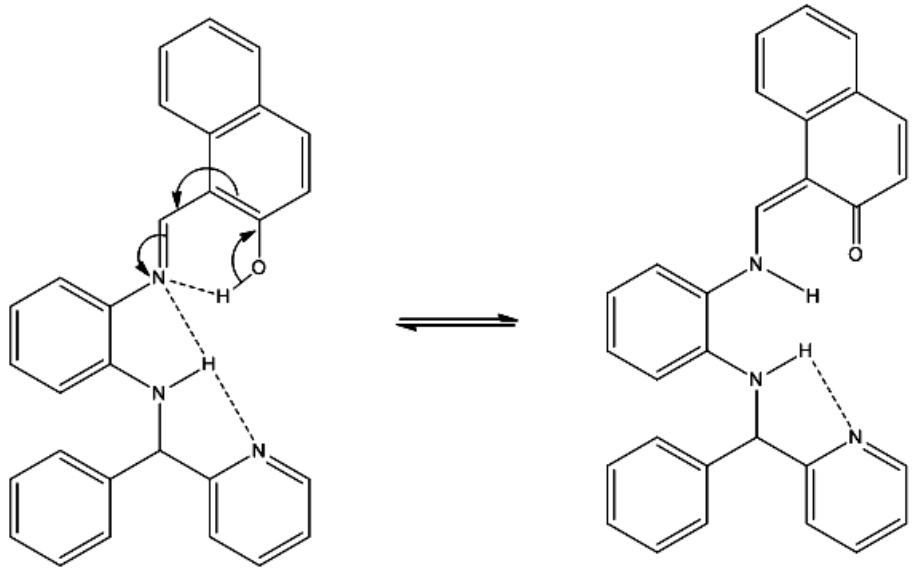

H-bonding
H_2L"

Scheme S2 Tautomerisation of **H_2L"** in excited state

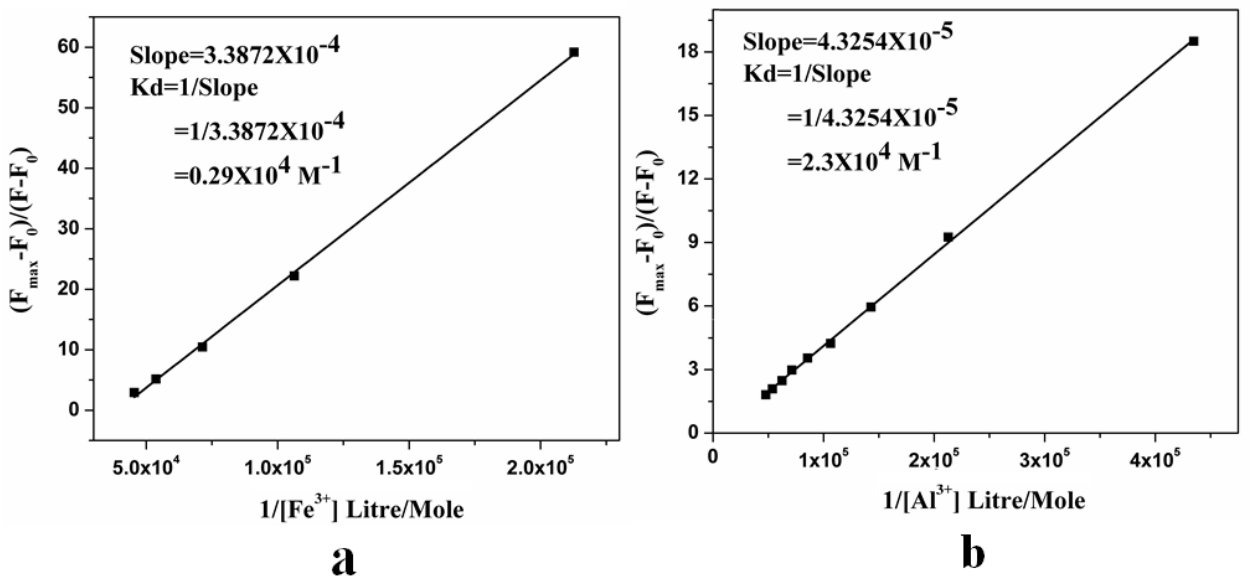

Fig. S17. Benesi-Hildebrand plot for determination of binding constant of probes with metal ions in H_2O (HEPES buffer, pH 7.4) (a) **HL'** with Fe^{3+} (b) **H_2L"** with Al^{3+}.

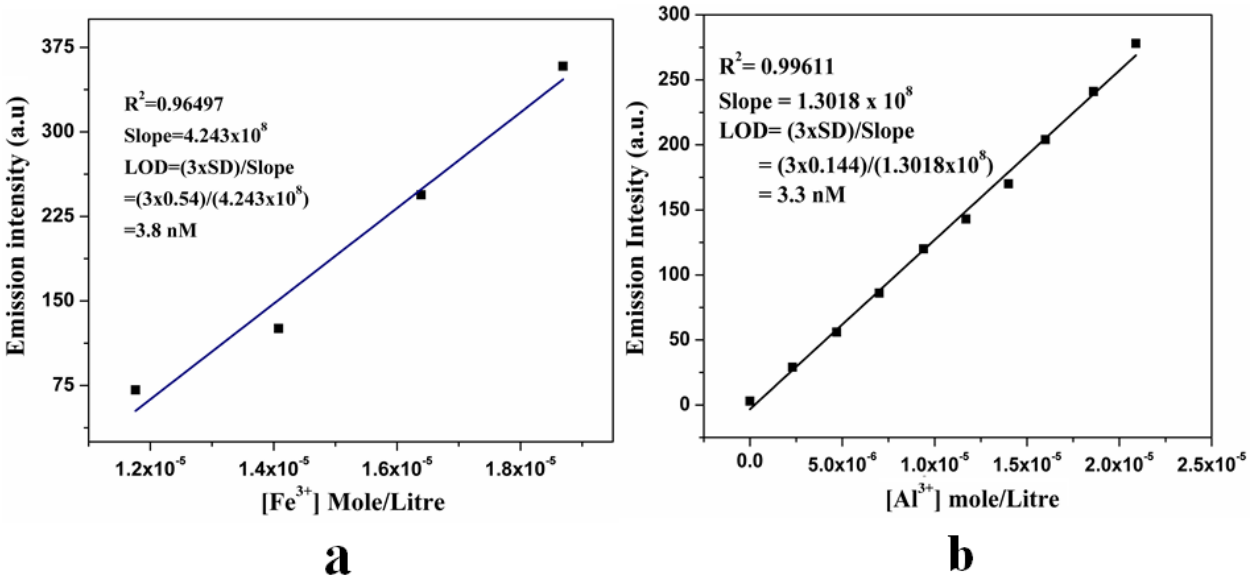

Fig. S18. LOD determination by following 3σ/m method (a) Fe^{3+} for probe **HL'** (b) Al^{3+} for **H_2L"**.

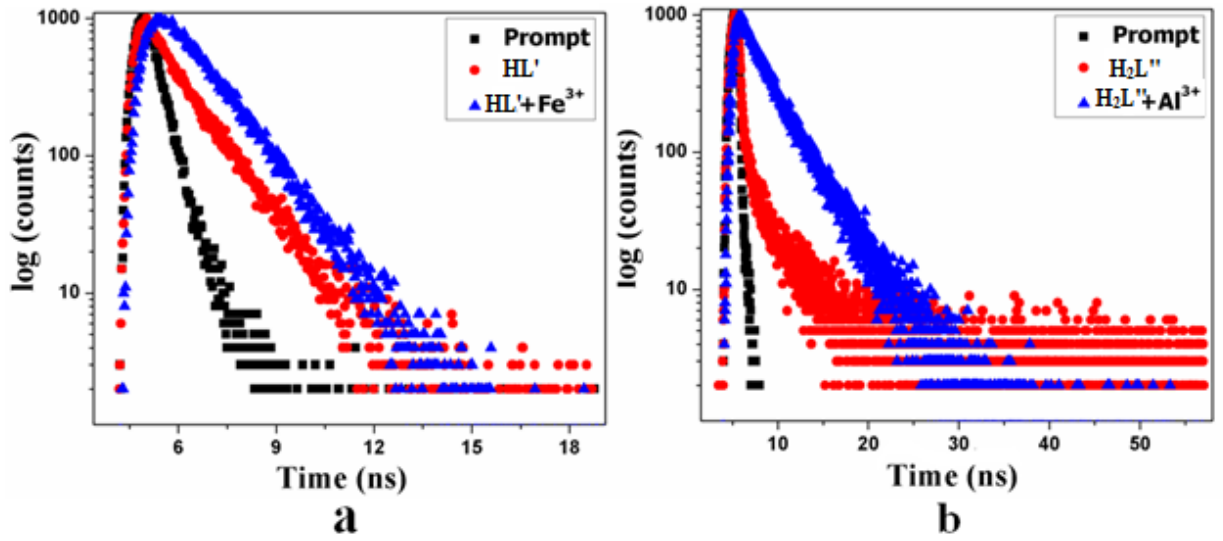

Fig. S19. Fluorescence lifetime spectra in H_2O (HEPES buffer, pH 7.4) (a) **HL'** and **HL'** with Fe^{3+} (b) **H_2L"** and **H_2L"** with Al^{3+}.

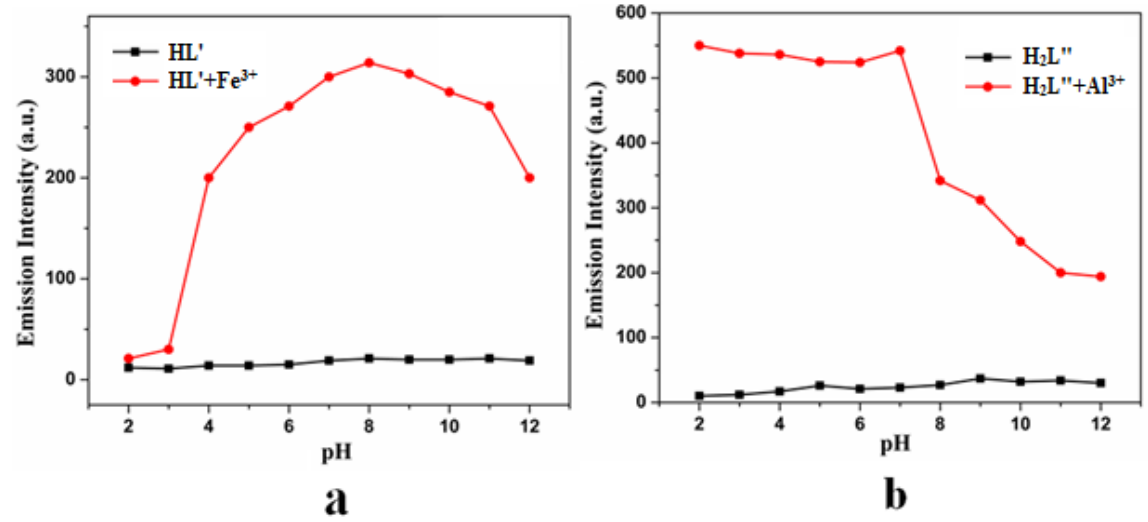

Fig. S20. Dependence of emission intensity for the probes on pH in the absence and presence of selective metal ions in H_2O (HEPES buffer, pH 7.4) (a) **HL'** and **HL'** with Fe^{3+} (b) **H_2L"** and **H_2L"** with Al^{3+}.

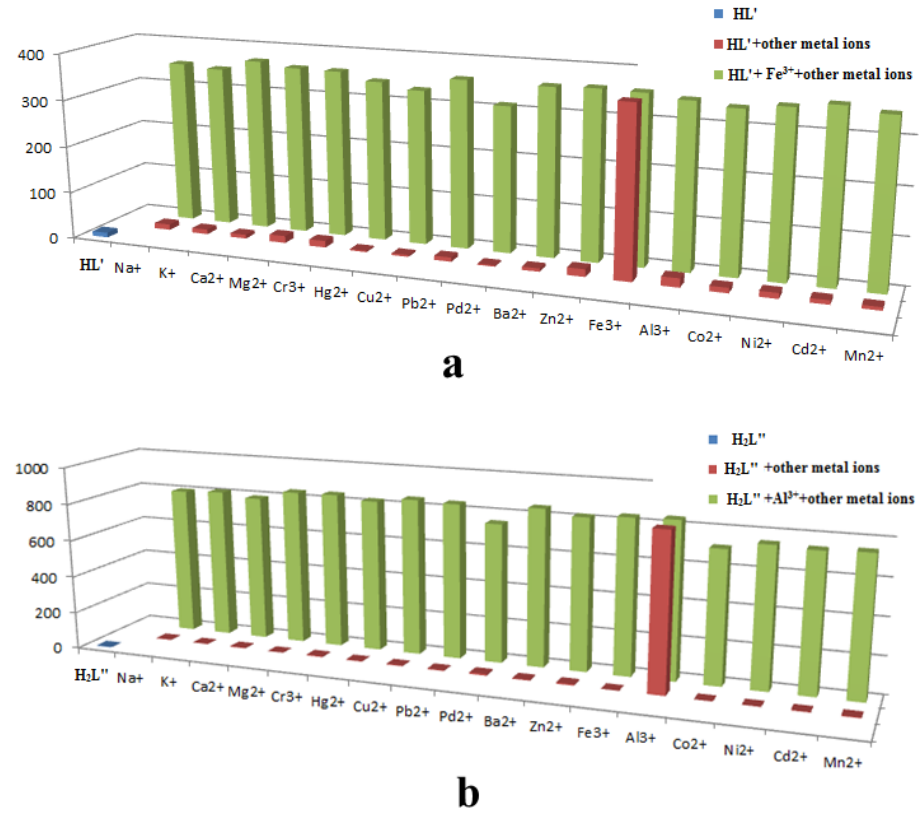

Fig. S21. Interference of various metal ions (a) Fe^{3+} sensitivity for **HL'** (b) Al^{3+} for **H_2L"**.

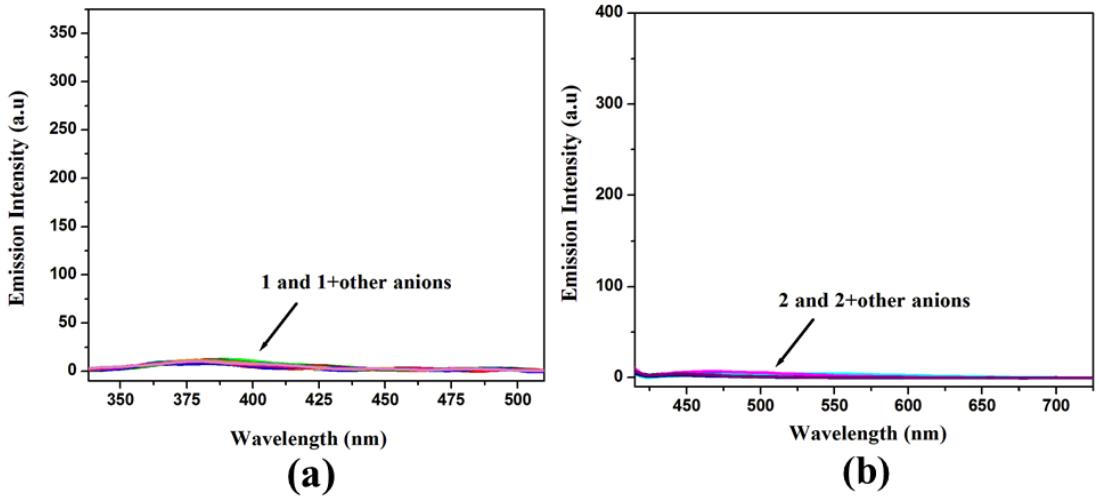

Fig. S22. Emission spectral changes of probes (50 μM) upon addition of various anions (100 μM) in H_2O (HEPES buffer, pH 7.4) (a) **HL'**, λ_{ex}=300 nm; (b) **H_2L"**, λ_{ex}=400 nm.

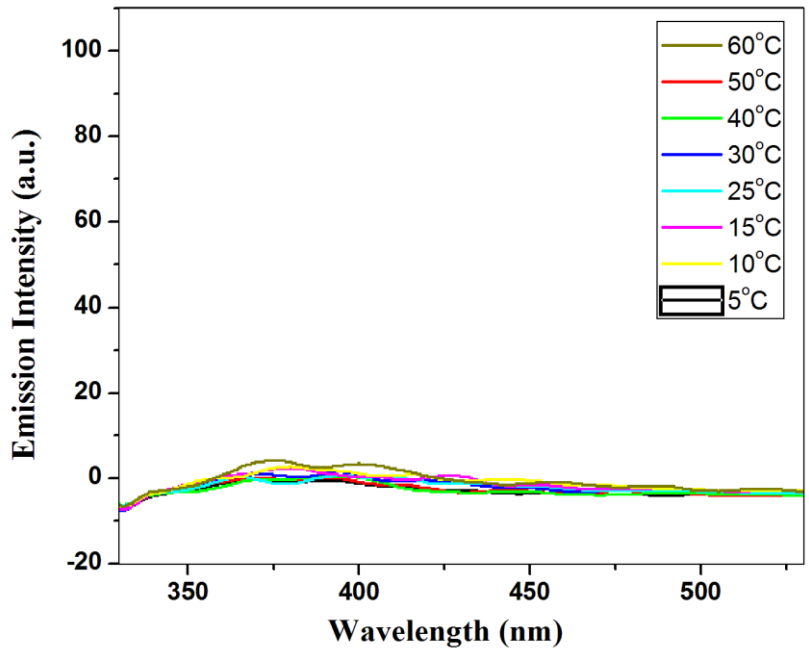

Fig. S23. Effect of temperature in fluorescence intensity of **HL'**.

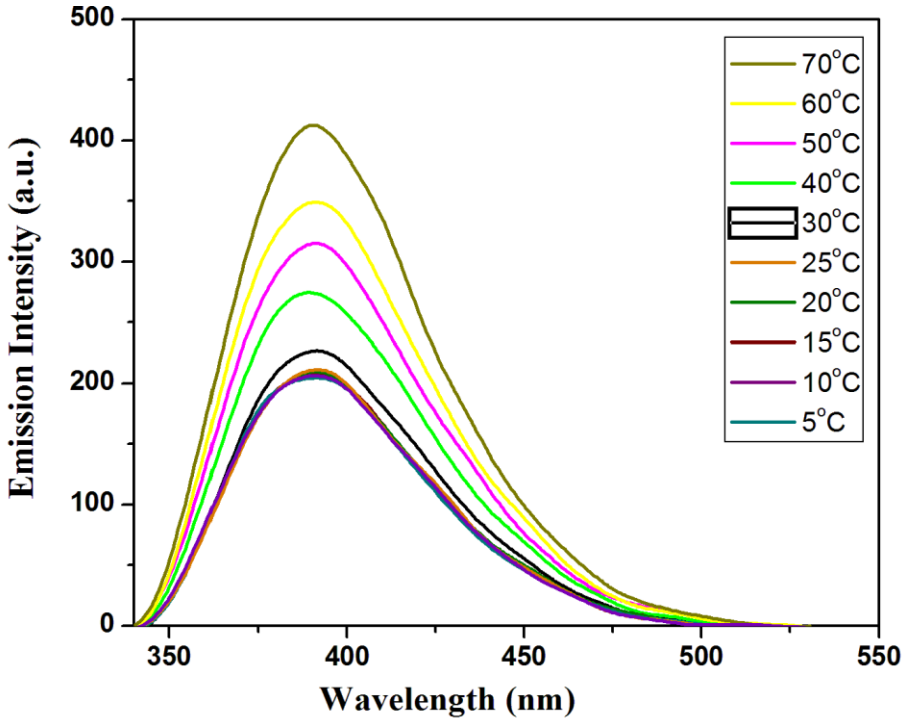

Fig. S24. Effect of temperature in fluorescence intensity of **HL'**+Fe^{3+}.

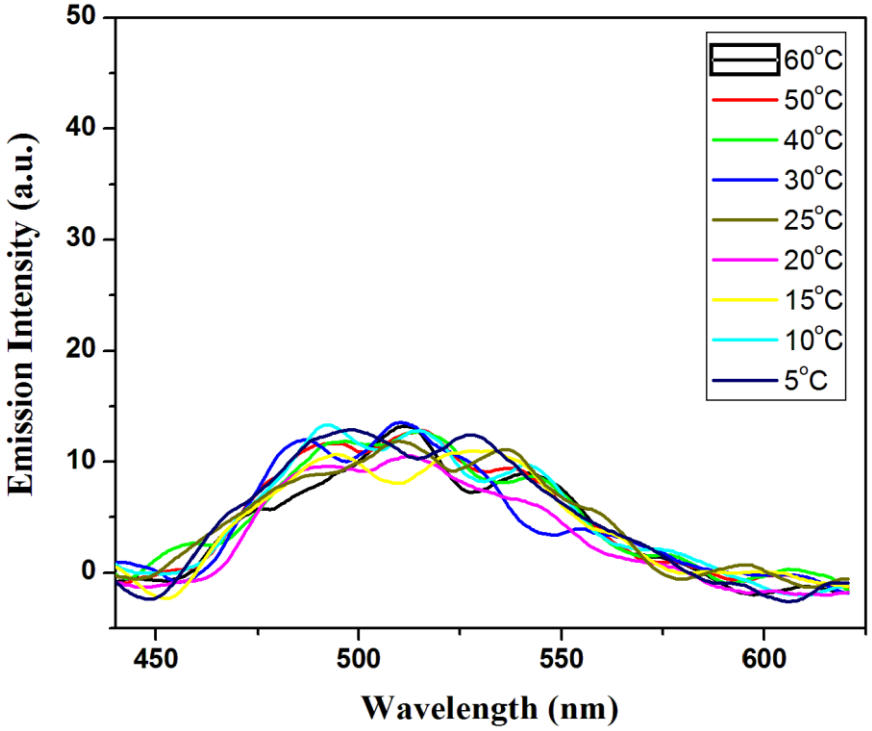

Fig. S25. Effect of temperature in fluorescence intensity of **H_2L''**.

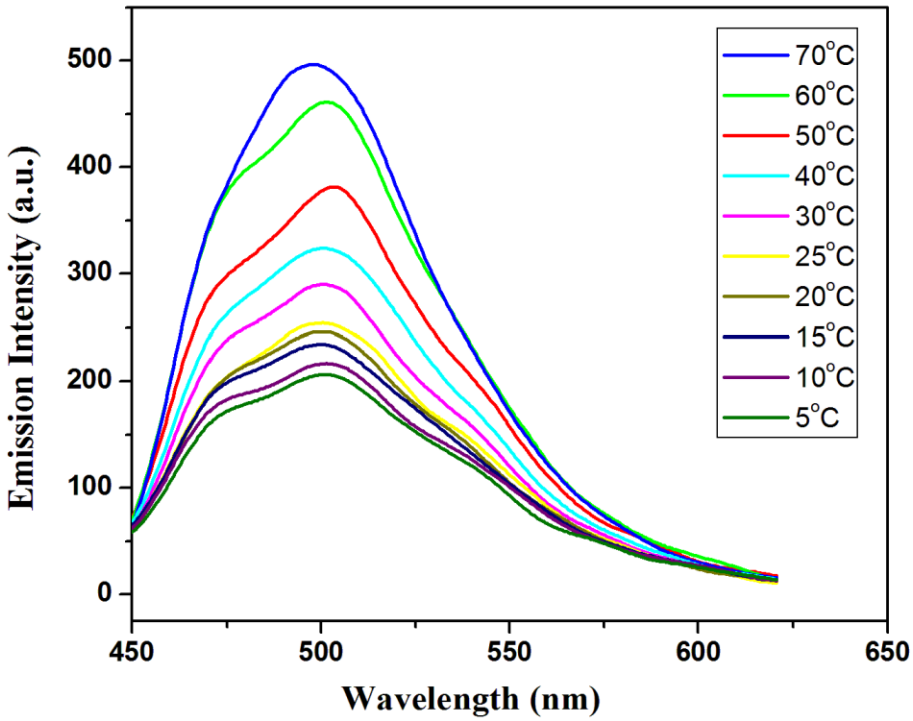

Fig. S26. Effect of temperature in fluorescence intensity of $\mathbf{H_2L''}$+Al^{3+}.

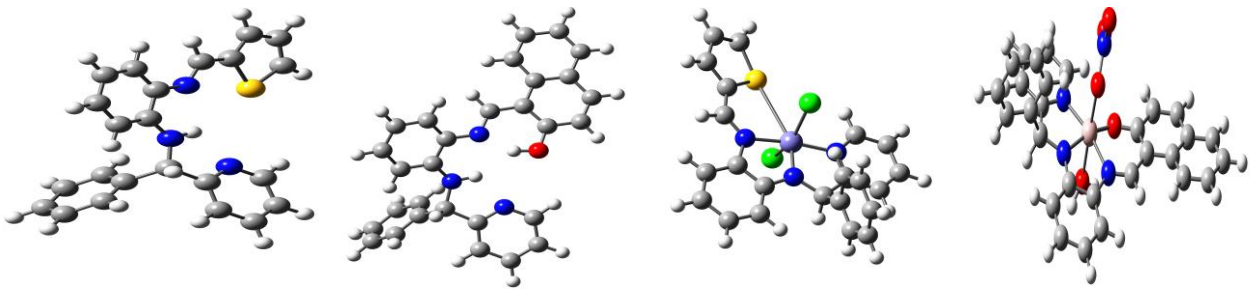

(a) (b) (c) (d)

Fig. S27. DFT-Optimized structures (a) **HL'**, (b) $\mathbf{H_2L''}$, (c) [Fe(**L'**)(Cl)2] and (d) [Al(**L''**)(NO3)(OH2)].

Table S4 some frontier molecular orbitals and energies of the probe **HL'**.

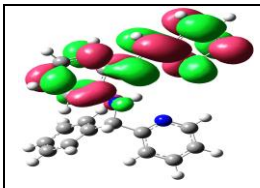	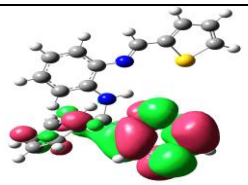	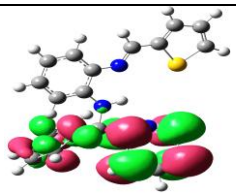	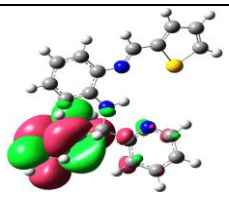	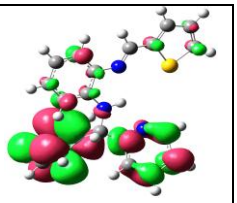
LUMO -1.63 eV	LUMO+1 -0.81 eV	LUMO+2 -0.57 eV	LUMO+3 0.03 eV	LUMO+4 0.17 eV
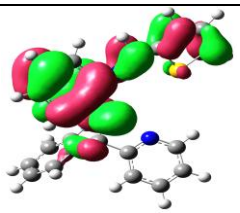	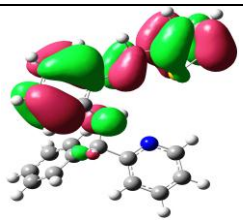	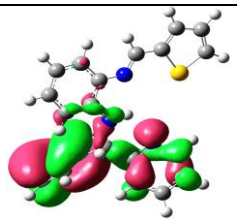	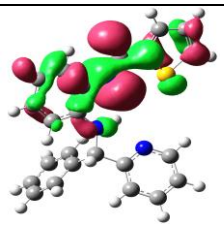	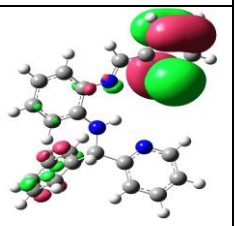
HOMO -4.74 eV	HOMO-1 -5.82 eV	HOMO-2 -6.51 eV	HOMO-3 -6.59 eV	HOMO-4 -6.76 eV

Table S5 some frontier molecular orbitals and energies of the probe **H_2L"**.

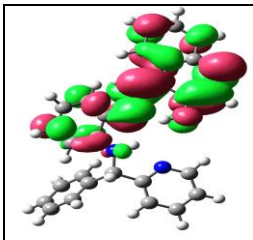	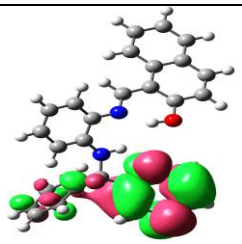	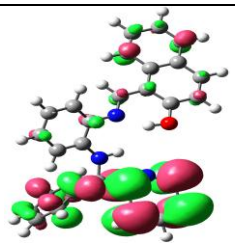	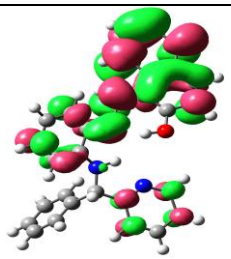	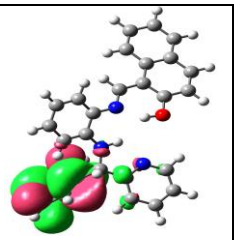
LUMO -1.69 eV	LUMO+1 -0.83 eV	LUMO+2 -0.58 eV	LUMO+3 -0.44 eV	LUMO+4 -0.07 eV
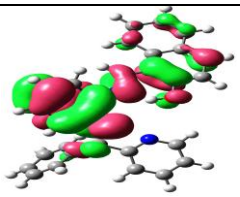	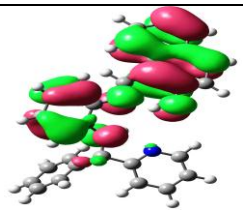	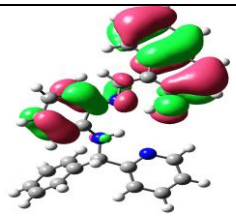	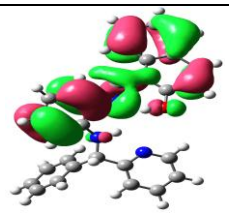	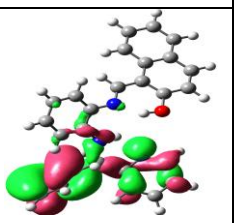
HOMO -4.85 eV	HOMO-1 -5.61 eV	HOMO-2 -6.24 eV	HOMO-3 -6.41 eV	HOMO-4 -6.6 eV

Table S6 some frontier molecular orbitals and energies of [Fe(**L'**)$(Cl)_2$] complex.

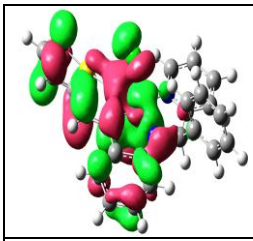	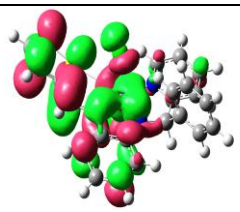	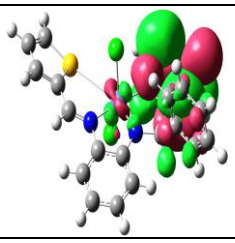	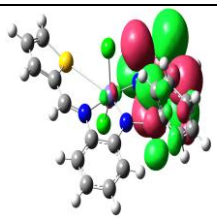	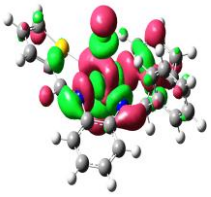
LUMO -2.61 eV	LUMO+1 -2.45 eV	LUMO+2 -1.63 eV	LUMO+3 -1.18 eV	LUMO+4 -1.0 eV
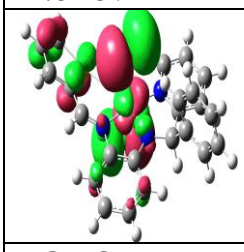	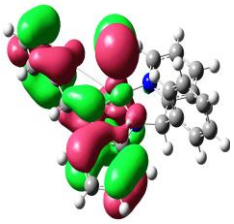	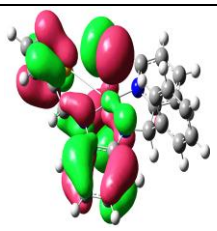	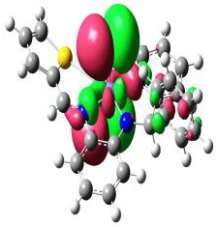	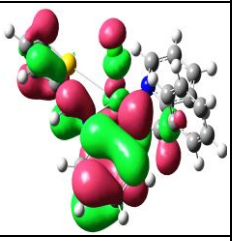
HOMO -5.27 eV	HOMO-1 -6.27 eV	HOMO-2 -6.42 eV	HOMO-3 -6.58 eV	HOMO-4 -6.64 eV

Table S7 some frontier molecular orbitals and energies of [Al(**L"**)$(NO_3)(OH_2)$] complex.

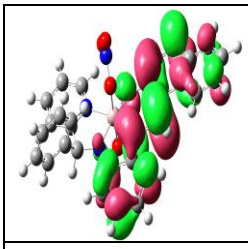	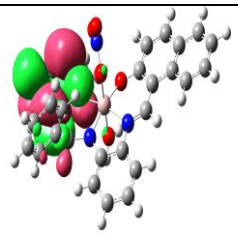	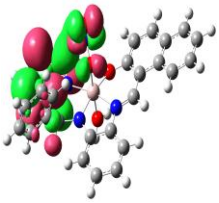	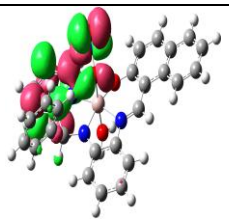	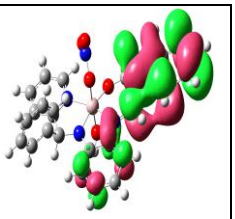
LUMO -2.28 eV	LUMO+1 -1.69 eV	LUMO+2 -1.09 eV	LUMO+3 -0.85 eV	LUMO+4 -0.67 eV
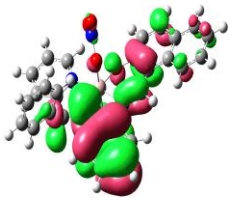	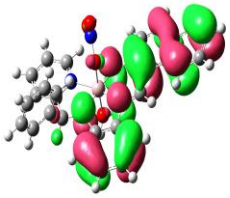	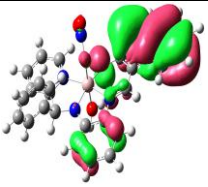	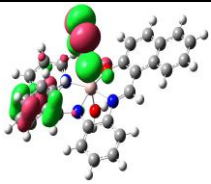	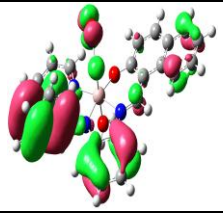
HOMO -5.35 eV	HOMO-1 -5.8 eV	HOMO-2 -6.27 eV	HOMO-3 -6.42 eV	HOMO-4 -6.76 eV

Table S8 Optimized coordinates for **HL'**

Center Number	Atomic Number	Coordinates (Angstroms)		
		X	Y	Z
1	16	2.219276	11.803553	8.827920
2	7	5.175970	12.753080	9.088510
3	7	5.955746	13.367159	6.596013
4	1	5.015842	13.091642	6.866363
5	7	3.717394	13.337891	5.227950
6	6	6.897323	13.476279	7.586794
7	6	7.046194	12.737626	4.429913
8	6	6.148715	13.719278	5.205655
9	1	6.618151	14.714698	5.131660
10	6	6.509617	13.164631	8.931778
11	6	4.771031	13.814632	4.535284
12	6	4.587424	12.545216	10.223809
13	1	5.082062	12.693843	11.192260
14	6	8.226990	13.893566	7.347260
15	1	8.547384	14.110551	6.335943
16	6	8.023230	13.213888	3.543746
17	1	8.173742	14.285692	3.433830
18	6	3.221591	12.102988	10.315489
19	6	2.490952	11.844970	11.455775
20	1	2.908525	11.961613	12.449268
21	6	6.877154	11.352740	4.580390
22	1	6.133052	10.984012	5.278880
23	6	9.138101	13.998769	8.396047
24	1	10.154890	14.316050	8.184576
25	6	4.621758	14.367210	3.254303
26	1	5.487781	14.732831	2.713725
27	6	7.456322	13.273339	9.965960
28	1	7.170098	13.017652	10.981688
29	6	8.817350	12.322394	2.811330
30	1	9.574811	12.704148	2.133568
31	6	8.762389	13.688222	9.712453
32	1	9.481020	13.760625	10.521701
33	6	7.669547	10.461491	3.851632
34	1	7.532736	9.391900	3.977740
35	6	0.836988	11.335439	9.880599
36	1	-0.094899	11.040629	9.423263
37	6	8.640518	10.943278	2.962978
38	1	9.257072	10.249266	2.400408
39	6	3.347247	14.427913	2.688013
40	1	3.207190	14.855625	1.700734
41	6	2.253374	13.931346	3.409871

42	1	1.249723	13.962510	3.001315
43	6	1.149408	11.413506	11.209911
44	1	0.447418	11.171119	11.998519
45	6	2.484916	13.393426	4.676098
46	1	1.677277	12.995963	5.280879

Table S9 Optimized coordinates for **H_2L''**

Center Number	Atomic Number	Coordinates (Angstroms)		
		X	Y	Z
1	8	13.944878	2.530119	13.646443
2	1	14.207706	1.902000	12.884851
3	7	14.181596	1.645746	11.248169
4	7	16.498686	0.269163	11.726642
5	1	16.158956	1.028645	12.308606
6	6	17.745507	0.025882	13.775648
7	6	13.525359	2.702114	10.835355
8	1	13.299807	2.806613	9.773327
9	6	13.078861	3.743238	11.734234
10	6	18.892571	-0.457437	11.568085
11	6	15.718969	-0.143728	10.669139
12	6	12.392711	4.924374	11.250140
13	6	14.520651	0.579762	10.380192
14	6	13.297816	3.605578	13.123109
15	6	17.564700	-0.499152	12.338951
16	1	17.265579	-1.559246	12.414555
17	6	11.940176	5.906818	12.196850
18	7	16.943984	1.044197	14.144723
19	6	16.054609	-1.241186	9.848544
20	1	16.973905	-1.783769	10.032911
21	6	12.182713	5.700379	13.588961
22	1	11.833544	6.450978	14.292187
23	6	12.841687	4.585890	14.041465
24	1	13.034213	4.415396	15.093802
25	6	19.657004	-1.622738	11.408648
26	1	19.284900	-2.567516	11.798721
27	6	12.138686	5.177691	9.872582
28	1	12.470881	4.474222	9.118724
29	6	19.371544	0.750458	11.038205
30	1	18.769927	1.647412	11.142551
31	6	15.233333	-1.613452	8.782598
32	1	15.514823	-2.463521	8.168606
33	6	11.262152	7.068766	11.741498

34	1	10.929564	7.794802	12.478304
35	6	13.708768	0.181348	9.306890
36	1	12.771964	0.701995	9.133434
37	6	11.475770	6.320160	9.458371
38	1	11.299582	6.482108	8.399480
39	6	18.675336	-0.534027	14.663216
40	1	19.324004	-1.340476	14.340476
41	6	11.028673	7.278698	10.396448
42	1	10.510099	8.169750	10.058662
43	6	21.361096	-0.374347	10.220222
44	1	22.311858	-0.340724	9.697612
45	6	14.055405	-0.908865	8.504964
46	1	13.408043	-1.213987	7.690021
47	6	20.597866	0.791871	10.369066
48	1	20.957818	1.731333	9.961055
49	6	20.887174	-1.583231	10.739731
50	1	21.466314	-2.493530	10.618564
51	6	17.913808	1.028280	16.342689
52	1	17.949831	1.441526	17.344183
53	6	18.755942	-0.025694	15.961914
54	1	19.464453	-0.445432	16.668460
55	6	17.020707	1.537780	15.399320
56	1	16.335992	2.346468	15.627499

Table S10 Optimized coordinates for [Fe(**L'**)$(Cl)_2$]

Center Number	Atomic Number	Coordinates (Angstroms)		
		X	Y	Z
1	7	9.025384	13.703105	2.522805
2	6	10.005583	14.220898	1.743977
3	1	10.276261	13.650844	0.863293
4	6	10.629995	15.430086	2.068966
5	1	11.413825	15.821431	1.429288
6	6	10.219031	16.114294	3.230520
7	1	10.685579	17.055388	3.508206
8	6	9.194640	15.571612	4.022462
9	1	8.838384	16.085255	4.909378
10	6	8.610558	14.352399	3.642452
11	6	6.315102	11.456406	4.174384
12	6	5.560627	11.524807	5.372272
13	1	5.601579	12.413742	5.990908
14	6	4.747198	10.447292	5.749005
15	1	4.172073	10.508434	6.669757
16	6	4.675183	9.283832	4.952604

17	1	4.057407	8.445629	5.262456
18	6	5.419438	9.203901	3.764547
19	1	5.381193	8.287569	3.182522
20	6	6.225847	10.284737	3.361358
21	7	7.045374	10.328169	2.186889
22	6	6.942885	9.415807	1.249159
23	1	6.151292	8.668128	1.334696
24	6	7.728756	9.255197	0.056110
25	6	7.363993	8.406088	-0.989614
26	1	6.454571	7.813645	-0.965339
27	6	8.273947	8.405632	-2.091968
28	1	8.135156	7.809707	-2.986778
29	6	9.355165	9.244443	-1.897109
30	1	10.193222	9.424339	-2.555957
31	16	9.302149	10.069862	-0.314829
32	17	9.957592	10.885515	3.034913
33	26	8.123610	11.999647	2.226608
34	6	6.277653	14.623668	4.554257
35	6	5.453362	14.884295	3.438216
36	6	6.012611	15.264917	5.780439
37	6	4.378259	15.781289	3.555660
38	1	5.652074	14.382456	2.493794
39	6	4.936823	16.166464	5.896135
40	1	6.637700	15.055422	6.648336
41	6	4.117453	16.427166	4.781777
42	1	3.744514	15.975984	2.693851
43	1	4.736404	16.654399	6.847223
44	1	3.283123	17.119364	4.867916
45	17	6.969476	12.883852	0.430478
46	6	7.481308	13.675000	4.417944
47	1	7.854692	13.446077	5.431763
48	7	7.174642	12.431809	3.698545

Table S11 Optimized coordinates for [Al(**L"**)(NO_3)(OH_2)]

Center Number	Atomic Number	Coordinates (Angstroms)		
		X	Y	Z
1	8	14.919515	2.867187	13.468966
2	7	16.645715	3.422025	11.413768
3	7	17.091983	0.867466	11.223827
4	6	16.431512	-0.994229	12.584541
5	6	16.422315	4.678726	11.757875
6	1	16.844934	5.457397	11.126901
7	6	15.652284	5.119204	12.898757

8	6	18.749979	-1.012600	11.584891
9	6	17.612094	1.602697	10.178172
10	6	15.581998	6.544041	13.218606
11	6	17.366920	3.023588	10.245531
12	6	14.914260	4.191190	13.700517
13	6	14.741826	6.982497	14.301846
14	7	15.805882	-0.000934	13.280009
15	6	18.331357	1.101069	9.059924
16	1	18.560901	0.042295	8.998911
17	6	14.006381	6.010238	15.058877
18	1	13.382895	6.354515	15.881686
19	6	14.091632	4.665343	14.773256
20	1	13.558427	3.918780	15.352937
21	6	19.610401	-0.266418	12.418207
22	1	19.250933	0.650218	12.879538
23	6	16.319696	7.550691	12.519845
24	1	17.000433	7.281352	11.719109
25	6	19.230058	-2.182641	10.962537
26	1	18.578218	-2.749903	10.297484
27	6	18.774449	1.969722	8.051207
28	1	19.328451	1.566164	7.206213
29	6	14.649816	8.367458	14.628059
30	1	14.006814	8.665744	15.453736
31	6	17.812741	3.875999	9.218657
32	1	17.613152	4.944090	9.260340
33	6	16.213684	8.898675	12.855275
34	1	16.793156	9.635419	12.303885
35	6	16.291816	-2.335398	12.981207
36	1	16.815118	-3.112075	12.433759
37	6	15.368400	9.320911	13.916757
38	1	15.296838	10.374929	14.171161
39	6	21.405486	-1.876030	12.016855
40	1	22.428394	-2.205509	12.184243
41	6	18.516239	3.356419	8.118471
42	1	18.859699	4.018451	7.328405
43	6	20.552951	-2.615969	11.175881
44	1	20.916326	-3.516614	10.685820
45	6	20.930064	-0.700294	12.632577
46	1	21.585694	-0.120107	13.277289
47	6	14.865510	-1.604369	14.807235
48	1	14.259075	-1.803577	15.684022
49	6	15.498040	-2.644269	14.097243
50	1	15.381655	-3.676714	14.415995
51	6	15.048470	-0.287135	14.373268
52	1	14.619479	0.563732	14.887407

53	13	16.140431	1.844422	12.537071
54	8	14.419786	1.552856	11.363814
55	1	13.639635	2.090083	11.596417
56	6	17.286762	-0.565235	11.374849
57	1	16.906775	-1.126557	10.498543
58	1	14.453074	1.247819	10.439970
59	7	17.763394	2.119800	15.086026
60	8	16.726789	1.770785	15.768025
61	8	18.893627	2.407066	15.592428
62	8	17.658557	2.170346	13.726010

Table S12 Electronic transition of **HL'**, **H_2L"**, [Fe(**L'**)$(Cl)_2$] and [Al(**L"**)$(NO_3)(OH_2)$] complex calculated by TDDFT/CPCM method.

Excitation energy (eV)	Wavelength Exp. (nm)	Wavelength Thro. (nm)	Oscillation Frequency (f)	Key Transitions	Nature of transition
HL'					
2.6862	460	461.55	f=0.3735	HOMO→LUMO, 49 %	ILCT
[Fe(**L'**)$(Cl)_2$]					
1.8821	640	658.77	f=0.0073	$H_{[\mathbf{HL}'(89)+Fe(6)+Cl(5)]} \rightarrow L{+}1_{[\mathbf{HL}'(97)+Fe(2)+Cl(1)]}$, (α), 99 %	ILCT
2.7556	460	449.93	f=0.0276	$H_{[\mathbf{HL}'(89)+Fe(6)+Cl(5)]} \rightarrow L{+}3_{[\mathbf{HL}'(99)+Fe(1)]}$, (α), 96 %	ILCT
H_2L"					
2.6639	428	465.43	f=0.3354	HOMO→LUMO, 49 %	ILCT
3.6784	324	337.06	f=0.0238	HOMO→LUMO+1, 48 %	ILCT
[Al(**L"**)$(NO_3)(OH_2)$]					
2.5624	438	483.86	f=0.1829	$H_{[\mathbf{H2L}''(97)+Al(1)+NO3(1)+H2O(1)]} \rightarrow L_{[\mathbf{H2L}''(99)]}$, 25 % $H_{[\mathbf{H2L}''(97)+Al(1)+NO3(1)+H2O(1)]} \rightarrow L{+}1_{[\mathbf{H2L}''(72)+Al(2)+NO3(25)+H2O(1)]}$, 25 %	ILCT
3.7980	323	326.44	f=0.0075	$H_{[\mathbf{H2L}''(97)+Al(1)+NO3(1)+H2O(1)]} \rightarrow L{+}3_{[\mathbf{H2L}''(53)+Al(1)+NO3(2)+H2O(44)]}$, 47 %	ILCT

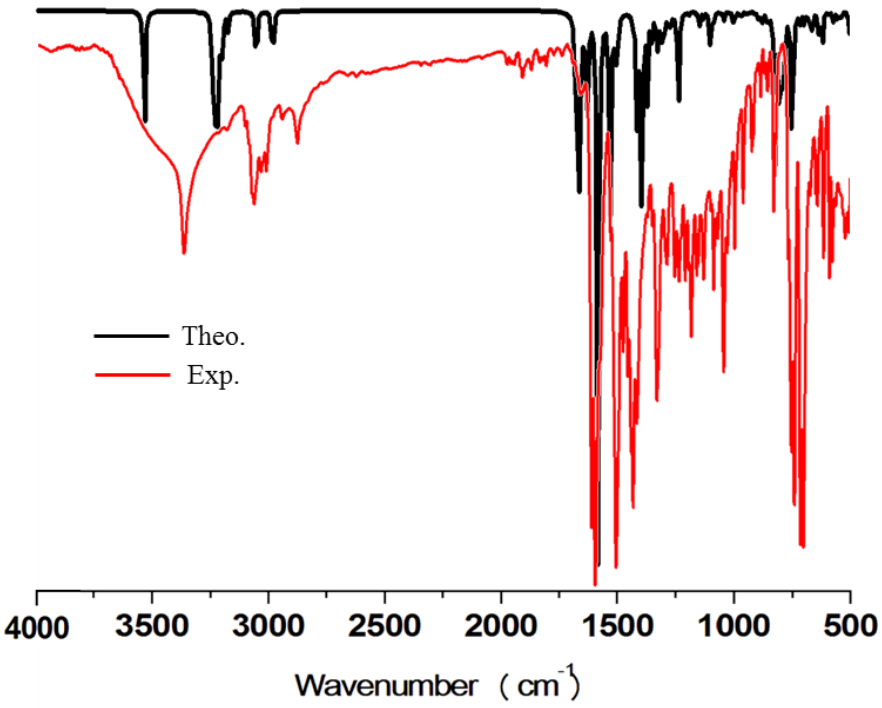

Fig. S28. Merged (experimental and theoretical) IR spectra of **HL'**.

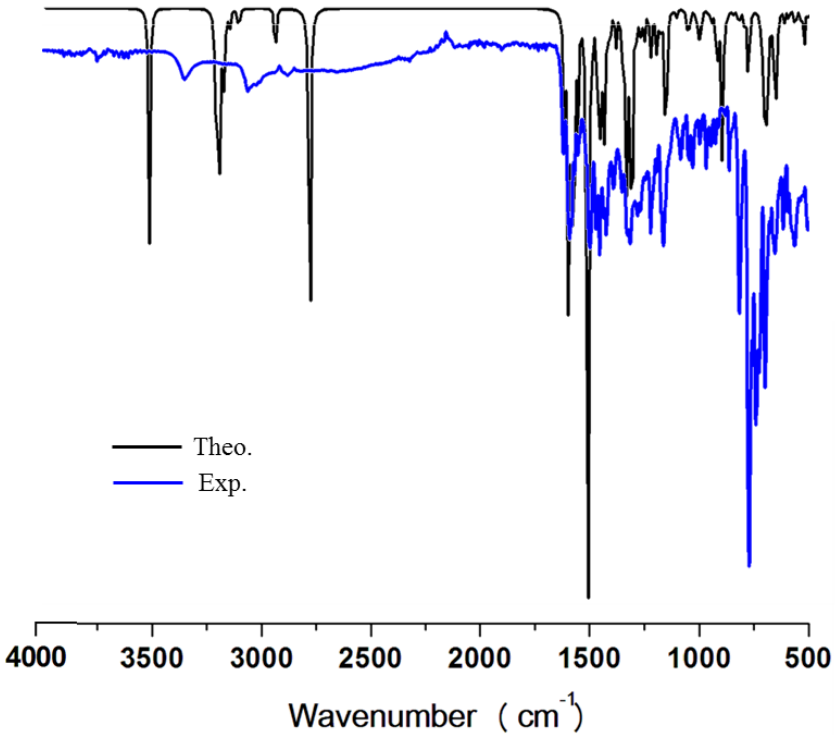

Fig. S29. Merged (experimental and theoretical) IR spectra of **H_2L''**.

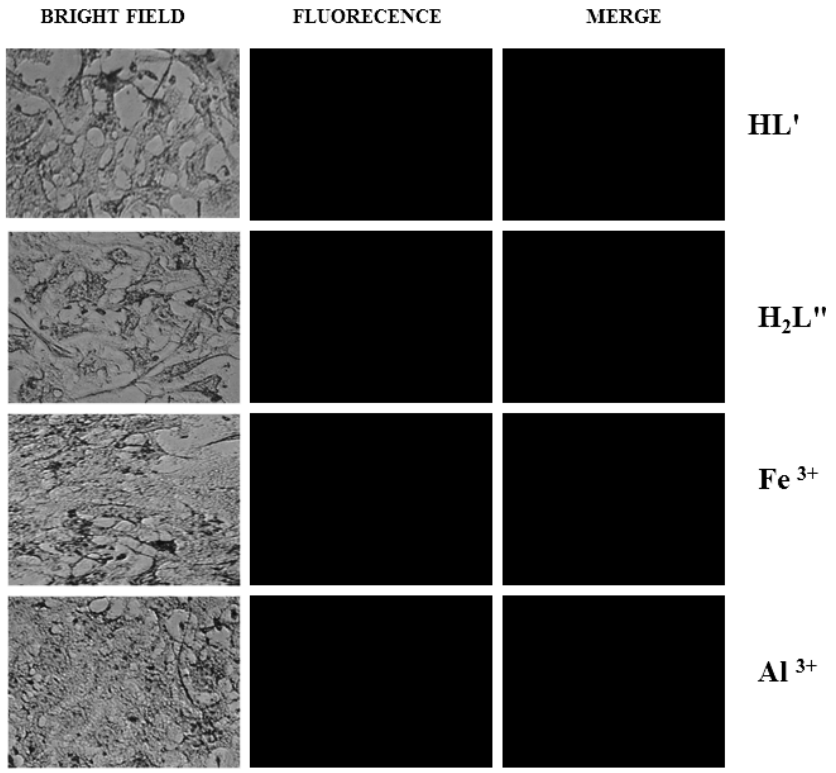

Fig. S30. Microscopic images of HepG2 cells treated with **HL'** (10 μM), **H_2L"** (10 μM), Fe^{3+} (10 μM) and Al^{3+} (10 μM) under bright, fluorescence and merged field.

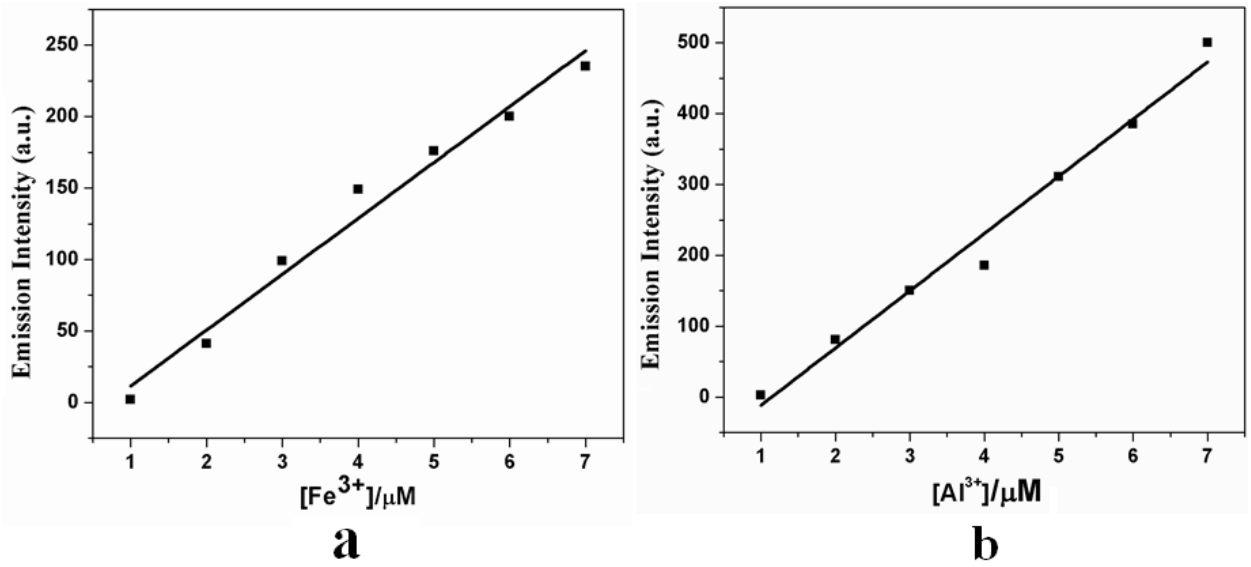

Fig. S31. Calibration plot for ion recovery (a) Fe^{3+} and (b) Al^{3+}.

Table S13 List of some reports with ion sensitivity

Sl. No	Probe	Selectivity (LOD)	Solvent	Application	Ref.
1.	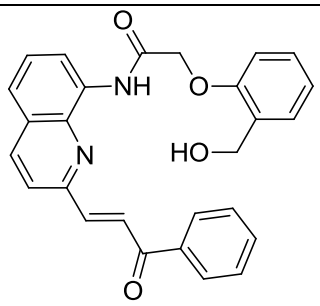	Fe^{3+} (2.68×10^{-7} M)	DMSO/ H_2O (5:1, pH 7.4)	Cell imaging	4
2.	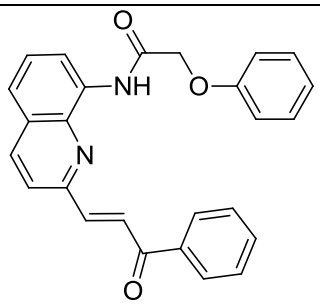	Fe^{3+} (5.11×10^{-8} M)	DMSO/ H_2O (5:1, pH 7.4)	Cell imaging	4
3.	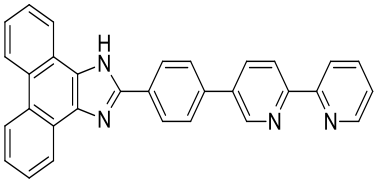	Fe^{3+} (5.26×10^{-6} M)	CH_3CN/ H_2O (1:1)	Fe^{3+} analysis in water sample	5
4.	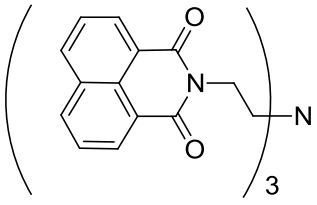	Fe^{3+} (4.69×10^{-7} M)	DMF/H_2O (2:3, v/v)	NO	6

5.	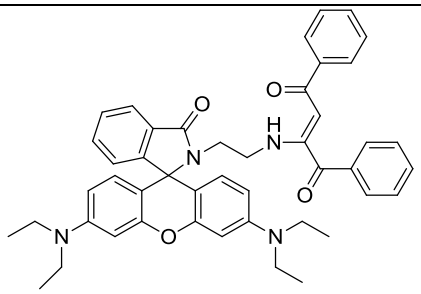	Fe^{3+} (7.68×10^{-7} M)	EtOH/ water (9:1, v/v)	Cell imaging	7
6.	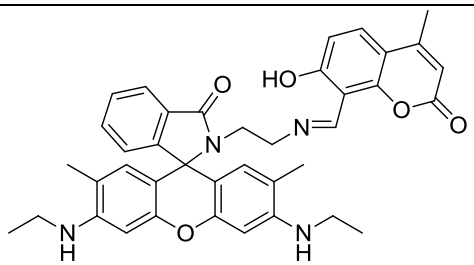	Fe^{3+} (5.6 ppb)	Ethanol	NO	8
7.	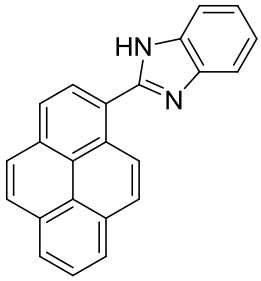	Fe^{3+} (11.2 ppb)	Water	NO	9
8.	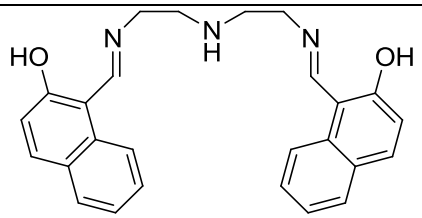	Al^{3+} (3.0×10^{-7} M)	ethanol/ water (3/7, v/v, pH 7.4)	Cell imaging	10
9.	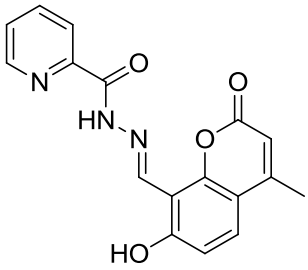	Al^{3+} (6.99×10^{-9} M)	Water	Electrical conductivity	11

10.	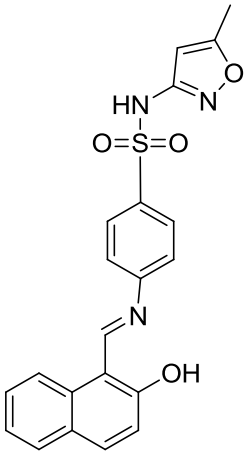	Al^{3+} (33.2×10^{-9} M)	MeOH-water (1 : 5)	Cell imaging, antibacterial and molecular docking	12
11.	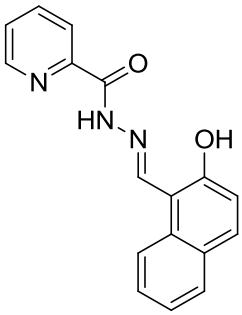	Al^{3+} (2.09×10^{-9} M)	Water	Cell imaging and paper strip	13
12.	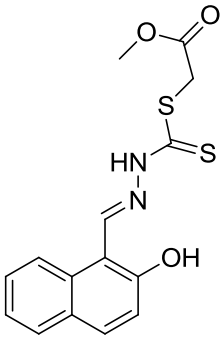	Al^{3+} (1.1×10^{-7} M)	MeOH/ H_2O (8:2)	NO	14
13.	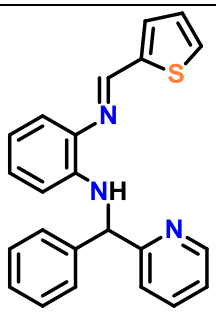	Fe^{3+} (3.8×10^{-9} M)	Water	Real water and cell imaging application	Present work

14.	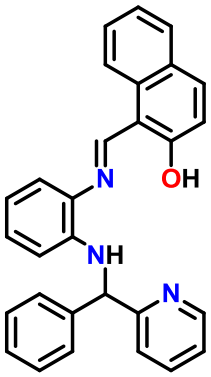	Al^{3+} (3.3×10^{-9} M)	Water	Real water and cell imaging application	Present work

References

1 D. D. Perrin, W. L. F. Armarego and D. R. Perrin, Purification of Laboratory Chemicals, Pergamon Press, Oxford, U.K., 1980.

2 A. Samui, K. Pal, P. Karmakar and S. K. Sahu, *Materials Science and Engineering C.*, 2019, **98**, 772-781.

3 K. Pal, S. Roy, P.K. Parida, A. Dutta, S. Bardhan, S. Das, K. Jana and P. Karmakar, *Materials Science and Engineering C.*, 2019, **95**, 204-216.

4 K. Xue, P. Wang, W. Dong, X. Luo, P. Cheng and K. Xu, *ChemistrySelect*, 2018, **3**, 11081-11086.

5 W. Lin, L. Long, L. Yuan, Z. Cao and J. Feng, *Anal. Chim. Acta*, 2009, **634**, 262-266.

6 L. Yang, W. Yang, D. Xu , Z. Zhang and A. Liu, *Dyes Pigments*, 2013, 97, 168-174.

7 Y. Hu, F. Zhao, S. Hu, Y. Dong, D. Li and Z. Su, *Journal of Photochemistry and Photobiology A: Chemistry*, 2017, **332**, 351-356.

8 J. An, T. Li, B. Wang, Z. Yang and M. Yan, *Journal of Coord. Chem.*, 2014, **67**, 921-928.

9 M. Zhao, Z. Deng, J. Tang, X. Zhou, Z. Chen, X. Li, L. Yanga and L-J Ma, *Analyst*, 2016, **141**, 2308-2312.

10 A. Sahana, A. Banerjee, S. Das, S. Lohar, D. Karak, B. Sarkar, S. K. Mukhopadhyay, A. K. Mukherjee and D. Das, *Org. Biomol. Chem.* 2011, **9**, 5523-5529.

11 R. Purkait, A. Dey, S. Dey, P. P. Ray and C. Sinha, *New J. Chem.*, 2019, **43**, 14979-14990.

12 S. Mondal, A. K. Bhanja, D. Ojha, T. K. Mondal, D. Chattopadhyay and C. Sinha, *RSC Adv.*, 2015, **5**, 73626-73638.

13 S. Dey, R. Purkait, K. Pal, K. Jana and C. Sinha, *ACS Omega*, 2019, **4**, 8451-8464.

14 V. Kumar, S. Kundu, B. Sk and A. Patra, *New J. Chem.*, 2019, **43**, 18582-18589.